WS2-4-5

距離減衰式の特徴と適用範囲
Characteristic and applicable range of GMPEs

2017年3月25日
（株）大崎総合研究所
Ohsaki Research Institute, Inc.
宮腰　淳一
Jun`ichi Miyakoshi

検討目的と検討内容
Objective and contents

- 検討目的 Objective

  – PSHA評価で採用する距離減衰式を選定
  Selection of GMPE applied to Ikata site for PSHA

- 検討内容 Contents

  – 距離減衰式の特徴と適用範囲
  Characteristic and applicable range of GMPEs

  – 伊方サイトに適用する距離減衰式の選定
  Selection of GMPE applied to Ikata site

距離減衰式の特徴と適用範囲（1）

Characteristic and applicable range of GMPEs (1)

距離減衰式	データベースの対象地域	地震タイプ	主なパラメータ	Mの範囲	距離の範囲	地盤条件・種別	その他
耐専スペクトル [Noda et al. (2002)]	国内	主に太平洋沿岸の60km以浅の地震	Mjma 等価震源距離 Vs, Vp 地盤の卓越周期	M_J 5.5～7.0	28～202km （震源距離）	500≦Vs≦2700 m/s	NFRD効果を考慮可能 水平動・鉛直動を評価可能
Kanno et al. (2006)	主に国内	内陸 プレート間 プレート内	Mw 断層最短距離 震源深さ、Vs30	5.5～8.2	1～500km	100≦Vs30≦1400 m/s	Vs30による補正可能
Zhao et al. (2006)			Mw 断層最短距離 震源深さ	5.0～8.3	0.3～300km	Soft soil ～ Hard rock (Hard rock Vs=2000m/s)	
内山・翠川 (2006)	日本周辺		Mw 断層最短距離 震源深さ	5.5～8.3	300km以内	150≦Vs30≦750m/s	
片岡ほか (2006)	国内	内陸 海溝性	Mw 断層最短距離 短周期レベル	陸: 4.9～6.9 海: 5.2～8.2	250km以内	Ⅰ種、Ⅱ種、Ⅲ種地盤および工学的基盤 （Vs=700m/s程度）	
Si et al. (2013)	国内	内陸 海溝型	Mw 断層最短距離 震源深さ	5.5～9.1	0～300km	Hard rock Vs≧2000m/s	鉛直動も作成

距離減衰式の特徴と適用範囲（2）

Characteristic and applicable range of GMPEs (2)

距離減衰式	データベースの対象地域	地震タイプ	主なパラメータ	Mの範囲	距離の範囲	地盤条件・種別	その他
Abrahamson et al. (2014)	主に国外	内陸	Mw 断層最短距離 Vs30 断層上端深さ	3.0～8.5	0～300km	100≦Vs30≦2000m/s	Vs30による補正可能 国による違いを考慮
Boore et al. (2014)			Mw 断層面の地表投影面への最短距離、 Vs30	3.0～8.0 （横ずれ、逆） 3.0～7.0 （正断層）	0～400km	150≦Vs30≦1500m/s	Vs30による補正可能 国による違いを考慮
Campbell and Bozorgnia (2014)			Mw 断層最短距離 Vs30 断層上端深さ 断層傾斜角、震源深さ	8.5以下 （横） 8.0以下 （逆） 7.5以下 （正）	0～300km	150≦Vs30≦1500m/s	Vs30による補正可能 国による違いを考慮
Chiou and Youngs (2014)			Mw 断層最短距離 Vs30 断層上端深さ 傾斜角	3.5～8.5 （横ずれ） 3.5～8.0 （逆、正断層）	0～300km	180≦Vs30≦1500m/s	Vs30による補正可能 国による違いを考慮
Idriss (2014)			Mw 断層最短距離 Vs30	5～7.9	0.2～150km	450≦Vs30≦2000m/s	Vs30による補正可能

○上記の5つはNGA-West2のGMPE

距離減衰式の特徴と適用範囲（3）

Characteristic and applicable range of GMPEs (3)

距離減衰式	データベースの対象地域	地震タイプ	主なパラメータ	Mの範囲	距離の範囲	地盤条件・種別	その他
Morikawa and Fujiwara (2013)	主に国内	内陸 プレート間 プレート内	Mw 断層最短距離 震源深さ、Vs30	5.5～9.0	200km以内	100≦Vs30≦1400 m/s	異常震域の補正有 深部地盤の補正有 Vs30による補正
Abrahamson et al. (2016)	主に国外	プレート間 プレート内	Mw 断層最短距離 or 震央距離 震源深さ、Vs30	6.0～8.4 5.0～7.9	300km以内	90≦Vs30＜2000 m/s	前弧・背弧別 M9地震への 適用性検討
佐々木・伊藤 (2016)	国内	内陸 プレート間 プレート内	Mw 断層最短距離or 等価震源距離 断層中心深さ	4.6～9.0	約200km 以内	ダム基礎岩盤 （700～1500m/s）	鉛直動も作成
森川・藤原 (2014)	国内	プレート間		9.1			既存の距離減衰式の 南海トラフ地震への 適用性検討
大野 (2016)	国内	プレート間		9.0	約50～ 1000km		既存の距離減衰式の M9地震への 適用性検討
司・ほか (2016)	国内	プレート間		9.0	43～ 1065km		既存の距離減衰式の M9地震への 適用性検討

○上記の6つのGMPEを追加（WS1でのコメント対応）

Morikawa and Fujiwara (2013)

Table 1. Events of fault plane models added to our database. The hypocenter location is after the JMA.

Origin time [JST]	Mw	Lat. [N]	Lon. [E]	Dep. [km]	Type	Ref.
2004/09/05 19:07	7.2	33.03	136.80	38	III	[3]
2004/09/05 23:57	7.4	33.14	137.14	44	III	[3]
2004/09/07 08:29	6.5	33.21	137.29	41	III	[3]
2004/10/23 17:56	6.5	37.29	138.87	13	I	[4]
2004/10/23 18:11	5.7	37.25	138.83	12	I	[4]
2004/10/23 18:34	6.2	37.31	138.93	14	I	[4]
2004/10/27 10:40	5.8	37.29	139.03	12	I	[5]
2004/11/08 11:15	5.5	37.40	139.03	0	I	[5]
2004/11/29 03:32	7.0	42.95	145.28	48	II	[3]
2004/12/06 23:15	6.7	42.85	145.34	46	II	[3]
2005/03/20 10:53	6.5	33.74	130.18	9	I	[6]
2005/08/16 11:46	7.1	38.15	142.28	42	II	[7]
2007/03/25 09:41	6.7	37.22	136.69	11	I	[7]
2007/07/16 10:13	6.6	37.56	138.61	17	I	[8]
2008/05/08 01:02	6.2	36.23	141.95	60	II	[9]
2008/05/08 01:45	6.8	36.23	141.61	51	II	[9]
2008/06/14 08:43	6.9	39.03	140.88	8	I	[10]
2008/07/19 11:39	6.9	37.52	142.26	32	II	[9]
2008/07/24 00:26	6.8	39.73	141.64	108	III	[11]
2008/09/11 09:20	6.8	41.78	144.15	31	II	[9]
2009/08/11 05:07	6.2	34.79	138.50	23	III	[12]
2011/03/09 11:45	7.2	38.33	143.28	8	II	[13]
2011/03/11 14:46	9.0	35.60	141.50	24	II	[14]
2011/03/11 15:08	7.4	39.84	142.78	32	II	[13]
2011/03/11 15:15	7.8	36.11	141.27	43	II	[13]
2011/03/12 03:59	6.2	36.99	138.60	8	I	[13]
2011/03/15 22:31	5.9	35.31	138.71	14	I	[13]
2011/03/19 18:56	5.8	36.78	140.57	5	I	[13]
2011/04/07 23:32	7.1	38.20	141.92	66	III	[13]
2011/04/11 17:16	6.6	36.95	140.67	6	I	[13]
2011/04/12 14:07	5.8	37.05	140.64	15	I	[13]
2011/06/23 06:50	6.6	39.95	142.59	36	II	[13]
2011/07/10 09:57	7.0	38.03	143.51	34	III	[13]
2011/07/23 13:34	6.3	38.87	142.09	47	II	[13]
2011/07/25 03:51	6.2	37.71	141.63	46	II	[13]
2011/07/31 03:53	6.3	36.90	141.22	57	III	[13]
2011/08/01 23:58	5.8	34.71	138.55	23	III	[13]
2011/08/19 14:36	6.3	37.65	141.80	51	III	[13]
2011/09/17 04:26	6.6	40.26	143.09	7	II	[13]
2011/11/24 19:25	6.1	41.75	142.89	43	II	[13]

Type: I = crustal, II = subduction plate-boundary, III = subduction intra-plate Ref: Referred fault model

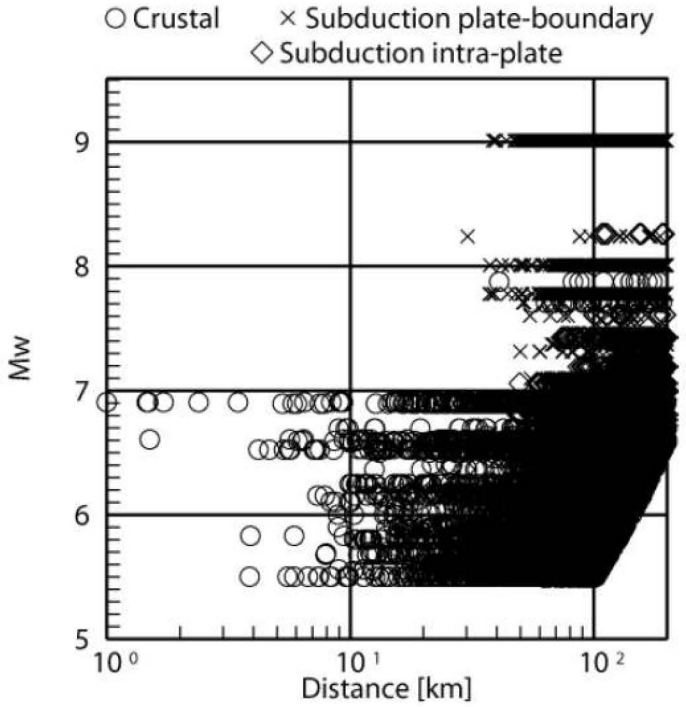

Fig. 1. Magnitude-distance distribution of strong-motion records used in regression analysis.

Kanno et al. (2006)に
追加した地震

Morikawa and Fujiwara (2013)

$$\log pre = a_1(Mw_1' - Mw_1)^2 + b_{1\_k}X + c_{1\_k} - \log(X + d_1 \cdot 10^{e_1 Mw_1'}) \pm \sigma_1 \quad . \quad (3)$$

$$Mw_1' = \min(Mw, Mw_{01}) \quad . \quad (4)$$

X：断層最短距離

Gd：深部地盤の補正項
Gs：浅部地震の補正項
AI：異常震域の補正項

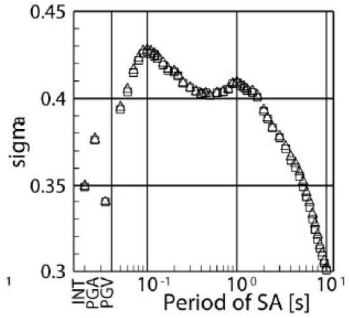

ばらつき
Standard deviation

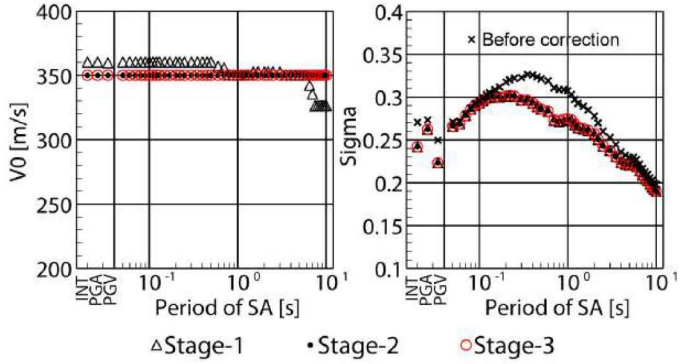

ばらつき

右上図：深部地盤補正後

右下図：浅部地盤補正後

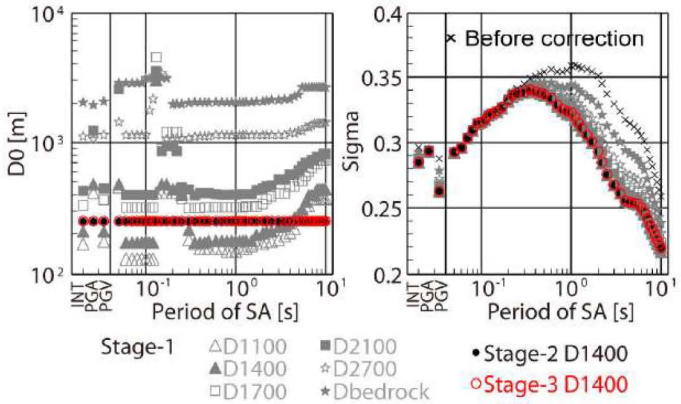

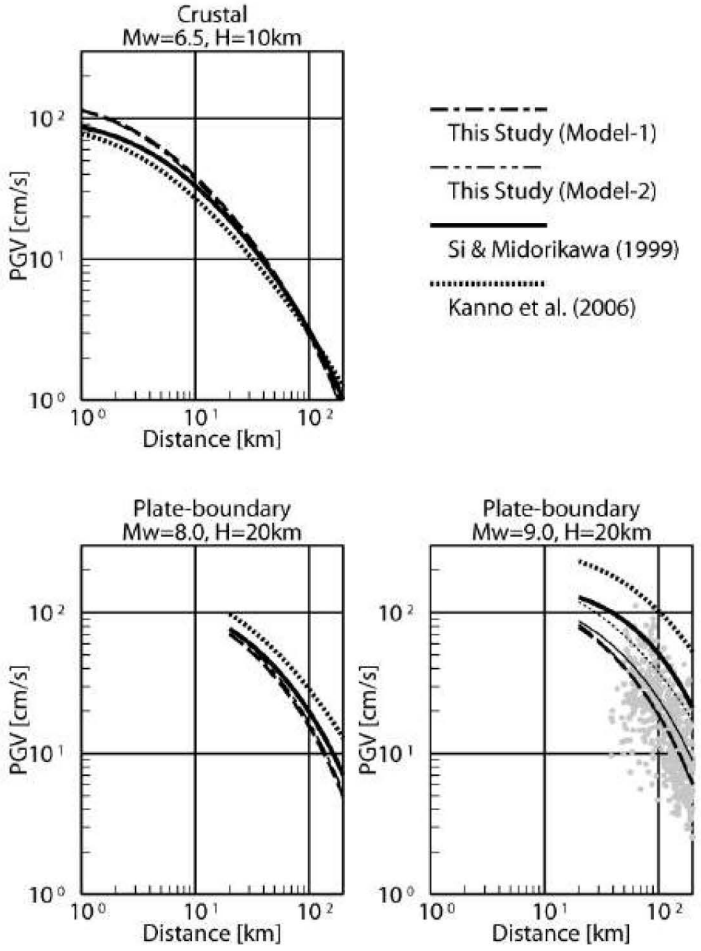

Fig. 10. Comparison of our new GMPE to existing Japanese GMPEs [1, 2] for PGV. *H* is the assumed focal depth required in the use of Si and Midorikawa's GMPE [1]. Thin lines in the right-lower panel are a case applying Mw = 8.2 instead of Mw = 9.0 for introducing magnitude saturation. Records observed during the 2011 earthquake are plotted using gray dots in the right-lower panel.

Abrahamson et al. (2016)

プレート間

$$\ln(Sa_{interface}) = \theta_1 + \theta_4\Delta C_1 + (\theta_2 + \theta_3(M-7.8))\ln(R_{rup} + C_4\exp(\theta_9(M-6))) + \theta_6 R_{rup} + f_{mag}(M) + f_{FABA}(R_{rup}) + f_{site}(PGA_{1100}, V_{S30}) \quad (1a)$$

震源補正項　前弧・背弧　サイト補正項

プレート内

$$\ln(Sa_{slab}) = \theta_1 + \theta_4\Delta C_1 + (\theta_2 + \theta_{14}F_{event} + \theta_3(M-7.8))\ln(R_{hypo} + C_4\exp(\theta_9(M-6))) + \theta_6 R_{hypo} + \theta_{10}F_{event} + f_{mag}(M) + f_{depth}(Z_h) + f_{FABA}(R_{hypo}) + f_{site}(PGA_{1100,V_{S30}}) \quad (1b)$$

ばらつき
Standard deviation

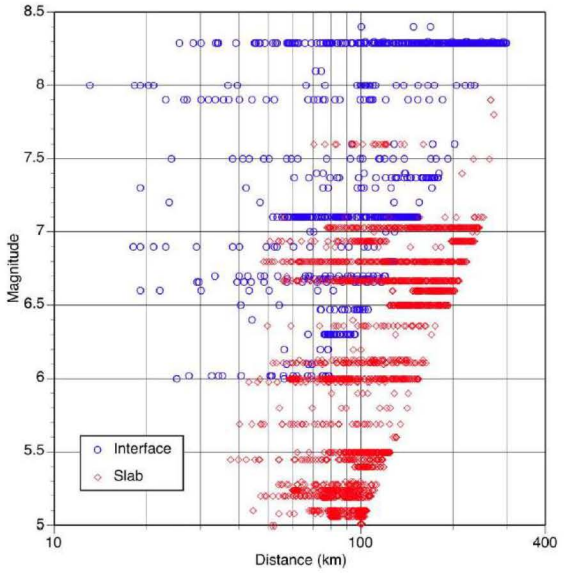

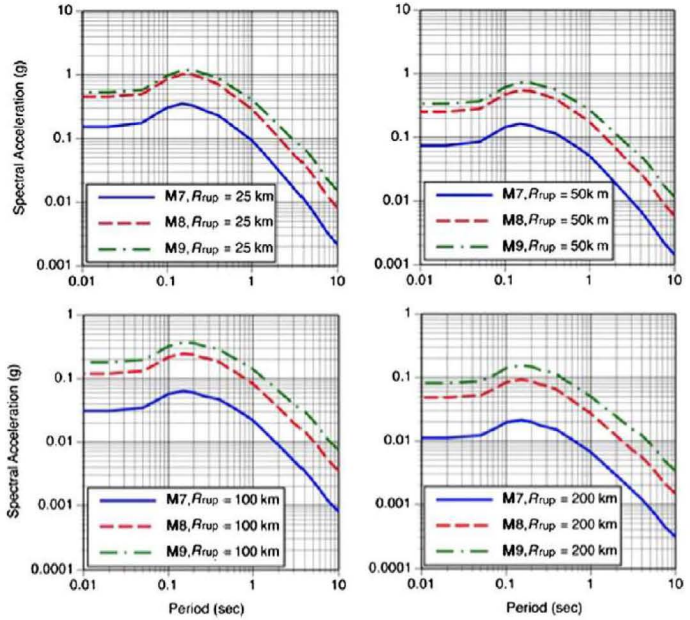

Figure 10. Examples of median spectra for interface earthquakes at sites with $V_{S30} = 760$ m/s located in the forearc region.

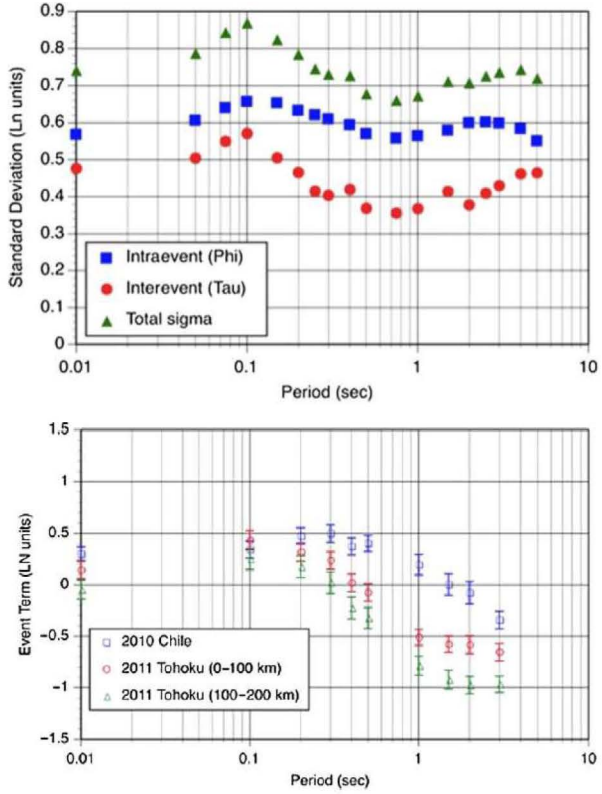

Figure 7. Event terms for the 2011 Tohoku, Japan, earthquake and the 2010 Maule, Chile, earthquake.

佐々木･伊藤(2016)

表-1　距離減衰式の回帰データ数

	対象期間	対象地震	ダム数	観測記録数	
				水平動	鉛直動
H13式	1974年～2000年	63地震	91ダム	293成分	―
H20式	1974年～2008年	88地震	213ダム	642成分	318成分
H23式	1974年～2011年	91地震	239ダム	794成分	394成分

表-2　地震種別の分類、加速度記録数

タイプ名（種別）	地震種別	解析対象の地震動観測記録数								
		地震数	観測記録数（水平動）				観測記録数（鉛直動）			
タイプA	内陸地殻内地震	37	288	組	456	成分	226	組	226	成分
タイプB	プレート境界地震	31	101	組	200	成分	99	組	99	成分
タイプα	プレート内地震	17	57	組	114	成分	57	組	57	成分
タイプE	日本海東縁部の地震	6	12	組	24	成分	12	組	12	成分

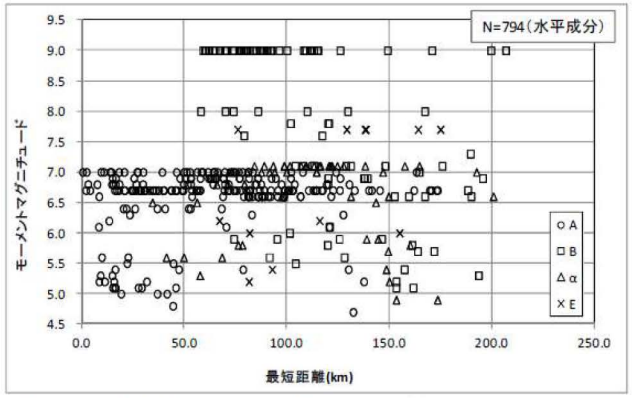

図-1　解析に用いた地震のマグニチュードと最短距離の関係

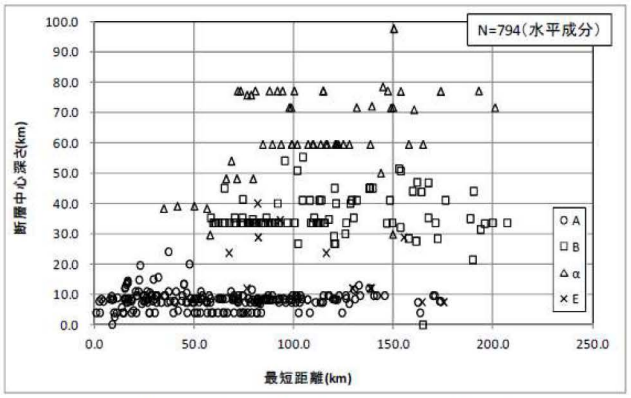

図-2　解析に用いた地震の断層中心深さと最短距離の関係

佐々木･伊藤(2016)

断層最短距離

$$logSA(T) = C_{m1}(T)M_W + C_h(T)H_C - \log(R + C_1(T)\cdot 10^{0.5M_W}) - (C_d(T) + C_{dh}(T)H_C)R + C_o(T) \quad (M_W \le 5.0)$$

$$logSA(T) = C_{m1}(T)M_W + C_{m2}(T)(M_o - M_W)^2 + C_h(T)H_C - log(R + C_1(T)\cdot 10^{0.5M_W}) - (C_d(T) + C_{dh}(T)H_C)R + C_o(T) \quad (M_o = 5.0, M_W > 5.0)$$

(1)

等価震源距離

$$logSA(T) = C_{m1}(T)M_W + C_h(T)H_C - \log\left(X_{eq} + C(T)\right) - (C_d(T) + C_{dh}(T)H_C)X_{eq} + C_o(T) \quad (M_W \le 5.0)$$

$$logSA(T) = C_{m1}(T)M_W + C_{m2}(T)(M_o - M_W)^2 + C_h(T)H_C - \log\left(X_{eq} + C(T)\right) - (C_d(T) + C_{dh}(T)H_C)X_{eq} + C_o(T) \quad (M_o = 5.0, M_W > 5.0)$$

(2)

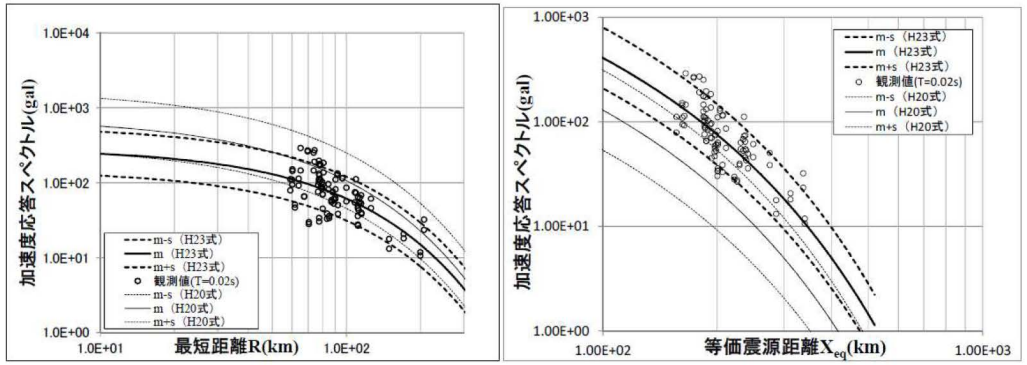

(a) 最短距離式　(b) 等価震源距離式

図-7　東北地方太平洋沖地震（2011. 3. 11、M_W9. 0）における基盤加速度の距離減衰特性

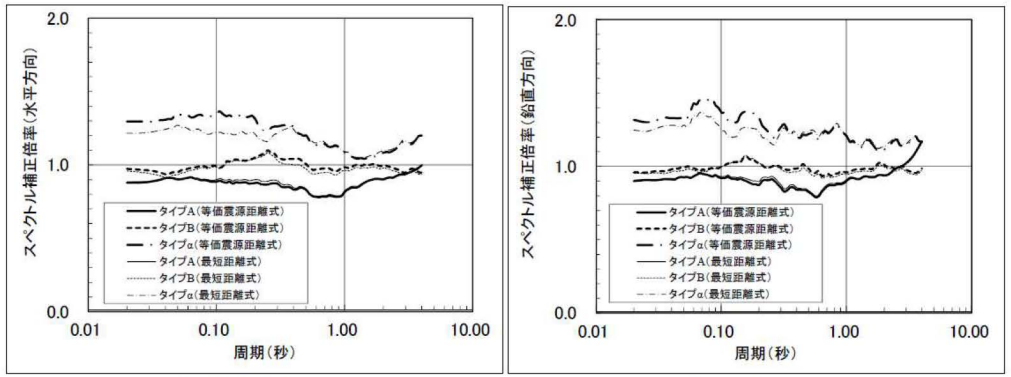

(a) 水平方向　(b) 鉛直方向

図-6　加速度応答倍率

ばらつきと
東北地方太平洋沖地震への適用性

地震タイプの違い
（全地震との比率）

距離減衰式の選定

Selection of GMPE applied to Ikata site

- 選定条件
  - 地盤条件 : Vs=2600m/s
  - 地震タイプ別に作成
  - 近距離への適用性
  - M9地震への適用性

- 選定候補となる距離減衰式
  - Zhao et al. (2006)
  - Si et al. (2013)
  - Morikawa and Fujiwara (2013)
  - Abrahamson et al. (2014)

参考文献
References

- Abrahamson, N., N. Gregor and K. Addo (2016): BC Hydro Ground Motion Prediction Equations for Subduction Earthquakes, Earthquake Spectra, Vol.32, No.1, 23–44.
- Abrahamson, A. A., W. J. Silva and R. Kamai (2014): Summary of the ASK14 Ground Motion Relation for Active Crustal Regions, Earthquake Spectra, 30, 1025-1055.
- Boore, D. M., J. P. Stewart, E. Seyhan and G. M. Atkinson (2014): NGA-West2 Equations for Predicting PGA, PGV, and 5% Damped PSA for Shallow Crustal Earthquakes, Earthquake Spectra, 30, 1075-1085.
- Campbell, K. W. and Y. Bozorgnia (2014): NGA-West2 Ground Motion Model for the Average Horizontal Components of PGA, PGV, and 5% Damped Linear Acceleration Response Spectra, Earthquake Spectra, 30, 1087-1115.
- Chiou, B. S.-J. and R. R. Youngs (2014): Update of the Chiou and Youngs NGA Model for the Average Horizontal Component of Peak Ground Motion and Response Spectra, Earthquake Spectra, 30, 1117-1153.
- Idriss, I. M. (2014): An NGA-West2 Empirical Model for Estimationg the Horizontal Spectral Values Generated by Shallow Crustal Earthquakes, Earthquake Spectra, 30, 1155-1177.
- 片岡正次郎・佐藤智美・松本俊輔・日下部毅明 (2006): 短周期レベルをパラメータとした地震動強さの距離減衰式, 土木学会論文集, Vol.62, No.4, 740-757.
- Knano, T., A. Narita, N. Morikawa, H. Fujiwara, and Y. Fukushima (2006): A New Attenuation Relation for Strong Ground Motion in Japan Based on Recorded Data, Bull. Seism. Soc. Am., Vol.96, No.3, 879-897.
- Morikawa, N. and H. Fujiwara (2013): A New Ground Motion Prediction Equation for Japan Applicable up to M9 Mega-Earthquake, Journal of Disaster Research, Vol.8, No.5, 878-888.
- 森川信之・藤原広行 (2014): 2011 年東北地方太平洋沖地震の観測記録に基づく地震動予測式と南海トラフ巨大地震への適用, 第14回日本地震工学シンポジウム論文集, 2711-2720.
- Noda, S., K. Yashiro, K. Takahashi, M. Takemura, S. Ohno, M. Tohdo, and T. Watanabe (2002): Response spectra for design purpose of stiff structures on rock sites, OECD/NEA Workshop.
- 大野晋 (2016): 東北地方太平洋沖地震の強震記録の距離減衰特性と地震動評価式の適用, 日本地震工学会論文集, 第16巻, 第4号, 2-11.
- 司宏俊・纐纈一起・三宅弘恵 (2016): プレート境界巨大地震の地震動距離減衰特性―伝播特性に着目した検討―, 日本地震工学会論文集, 第16巻, 第1号, 96-105.
- 佐々木隆・伊藤壮志 (2016): 東北地方太平洋沖地震を踏まえたダム基礎岩盤における地震動距離減衰式, 日本地震工学会論文集, 第16巻, 第4号, 80-92.
- Si, H., S. Midorikawa, H. Tsutsumi, C. Wu, T. Masatsuki, and A. Noda (2013): Preliminary analysis of attenuation relationship response spectra on bedrock based on strong motion records including the 2011 Mw9.0 Tohoku earthquake, Proceedings of 10th International Conference on Urban Earthquake Engineering, 113-117.
- 高橋克也・武村雅之・藤堂正喜・渡辺孝英・野田静男 (1998): 様々な岩盤上での強震動応答スペクトルの予測式, 第10回日本地震工学シンポジウム論文集, 547-552.
- 内山泰生・翠川三郎 (2006): 震源深さの影響を考慮した工学的基盤における応答スペクトルの距離減衰式, 日本建築学会構造系論文集, 第606号, 81-88.
- Zhao, J., J. Zhang, A. Asano, Y. Ohno, T. Oouchi, T. Takahashi, H. Ogawa, K. Irikura, H. K. Thio, P. G. Somerville, Y. Fukushima and Y. Fukushima (2006): Attenuation Relations of Strong Ground Motion in Japan Using Site Classification Based on Predominant Period, Bull. Seism. Soc. Am., Vol.96, No.3, 898-913.

【補足資料】

Noda et al.(2002)

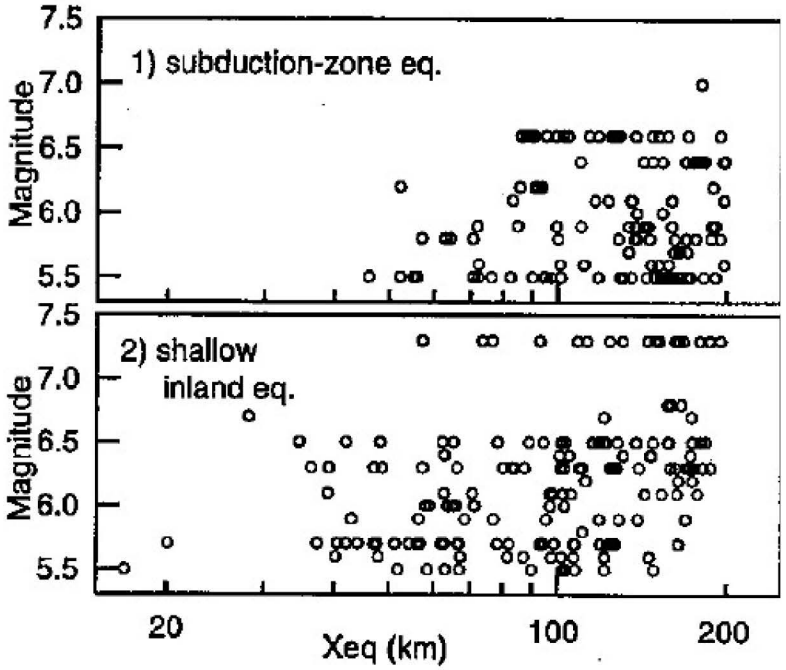

Fig. 6 M-Xeq distribution of the data used for analysis in Fig. 8.

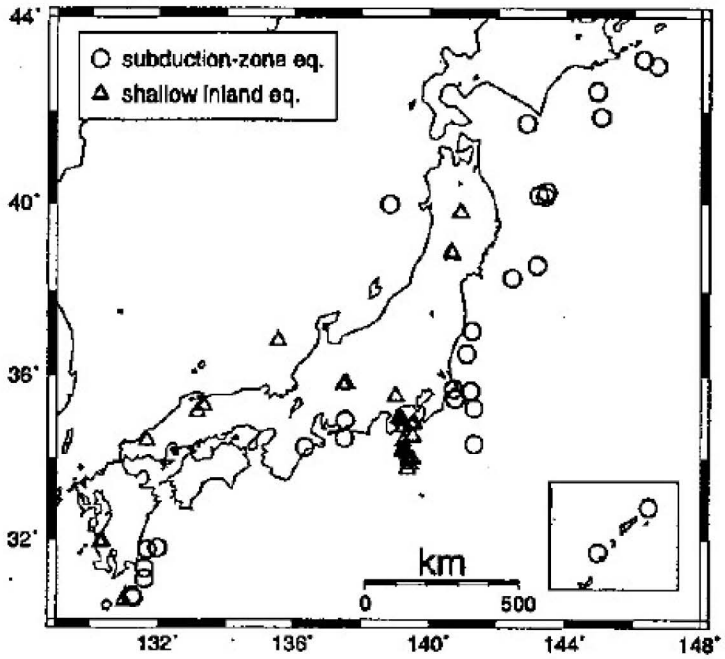

Fig. 7 Epicenter distribution of the earthquakes used for analysis in Fig. 8.

Table 3. Data Range used for analysis

	Data for regression analysis in Ref. 4,5	Data for applicability check in Ref.7	Data used in this paper	
			subduction-zone eq.	shallow inland eq.
Magnitude	5.5 - 7.0	5.4 - 8.1	5.5 - 7.0	5.5 - 7.3
Xeq (km)	28 - 202	14 - 218	46 - 199	17 - 195
Vs (m/s)	≥500	≥550	≥700	≥500
Number of Records	107	37	124	170

All data satisfy 1) Focal depth ≤ 60km, 2) Observation sites belong to stratum of tertiary or older.

Noda et al.(2002)

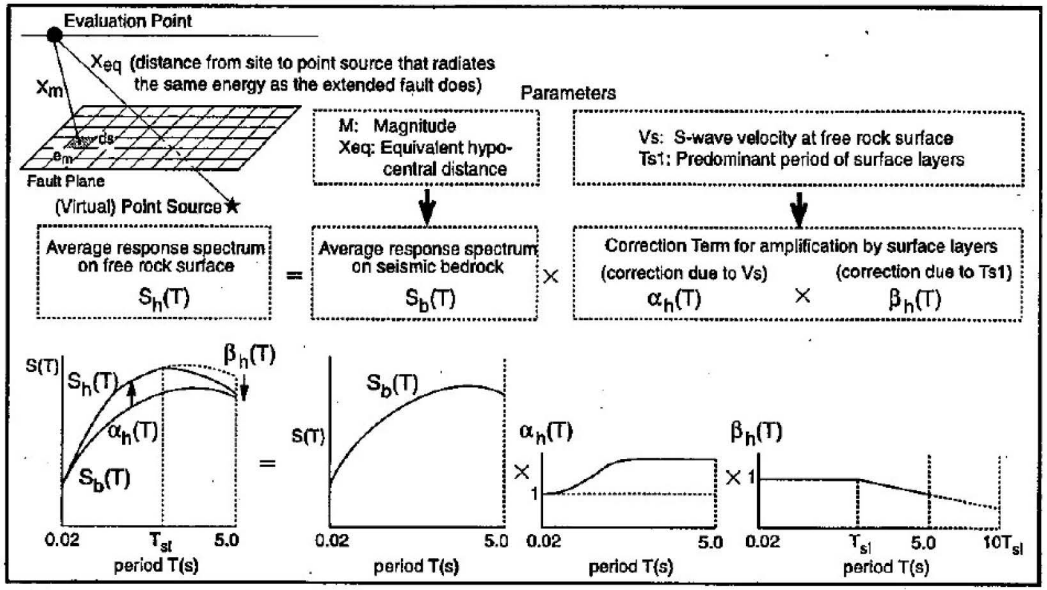

Fig.1 Evaluation Flowchart of Response Spectrum of Horizontal Ground Motion on Free Rock Surface

Xeq：等価震源距離

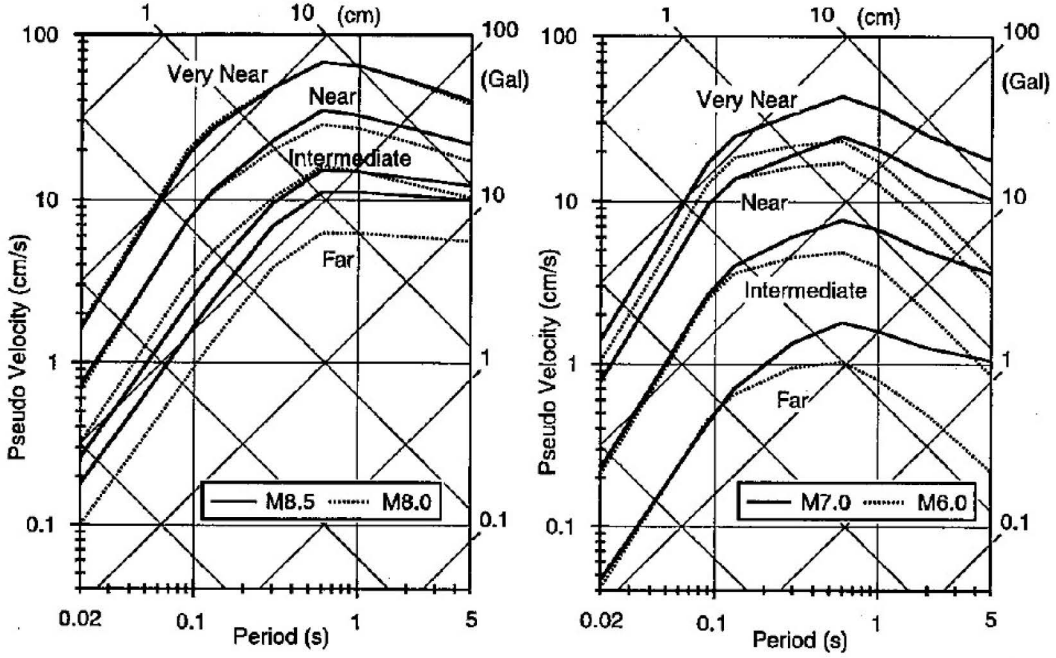

Fig. 2 Response Spectra of Horizontal Earthquake Motions on Seismic Bedrock at the Control Points in Table 1.

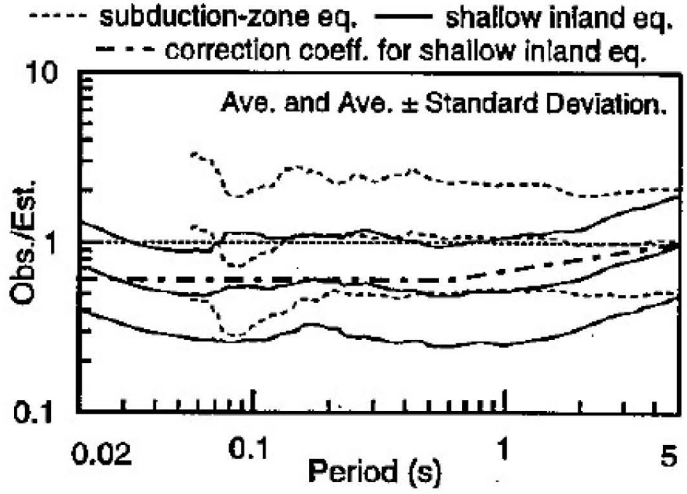

Fig. 8 Observation-to-Estimation Response Spectral Ratios

ばらつき
Standard deviation

Kanno et al.(2006)

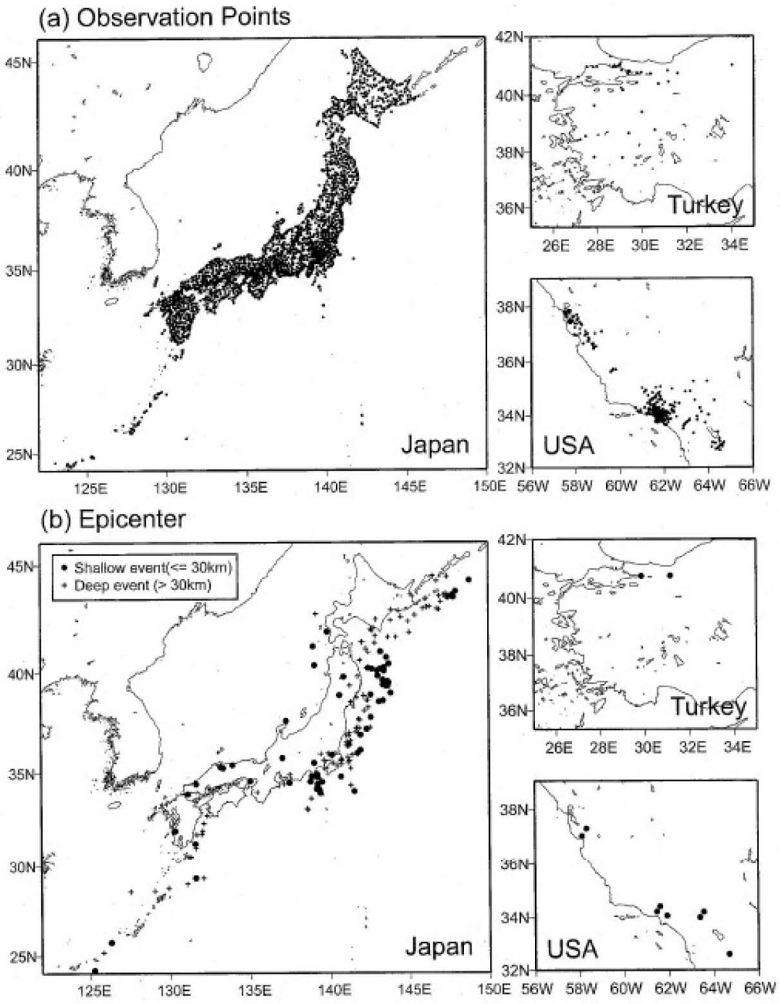

Figure 1. (a) Observation site locations and (b) epicenters of earthquakes used in regression analysis.

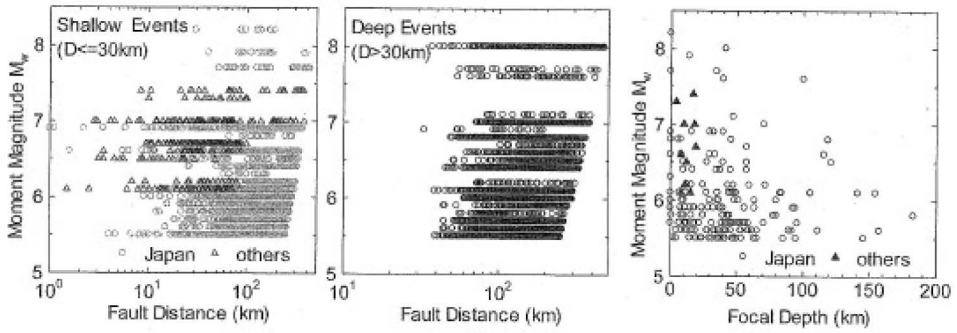

Figure 2. Magnitude–distance and magnitude–focal-depth distributions for PGA.

Table 1
Number of Data Used for Regression Analysis

	Shallow Events				Deep Events	
	Japan		Others		Japan	
Period	Data	Earthquake	Data	Earthquake	Data	Earthquake
PGA	3392	73	377	10	8150	111
5% Damped Acceleration Spectra (sec)						
0.05~1.00	3392	73	377	10	8150	111
1.10~1.20	3391	73	377	10	8145	111
1.30	3391	73	377	10	8144	111
1.50	3391	73	377	10	8140	111
1.70~2.00	3391	73	377	10	8137	111
2.20	3380	73	375	10	8100	111
2.50~3.00	3360	73	375	10	8039	110
3.50~4.00	3312	73	371	10	7963	110
4.50	3311	73	371	10	7963	110
5.00	3205	70	331	10	7721	101
PGV	2057	61	352	10	6490	110

Table 2
Earthquakes in Countries Other Than Japan Used for Regression Analysis

Source Region	Country	Origin Time (UT) (y/m/d h:m)	Focal Depth (km)	M_w
San Fernando	USA	1971/02/09 14:01	8.4	6.6
Imperial Valley	USA	1979/10/15 23:17	12.1	6.5
Morgan Hill	USA	1984/04/24 21:15	8.4	6.1
North Palm Springs	USA	1986/07/08 09:20	11.1	6.2
Whittier Narrows	USA	1987/10/01 14:42	14.7	6.1
Loma Prieta	USA	1989/10/18 00:04	17.6	7.0
Landers	USA	1992/06/28 11:58	4.5	7.3
Northridge	USA	1994/01/17 12:30	19.0	6.7
Kocaeli	Turkey	1999/08/17 00:01	17.0	7.4
Duzce	Turkey	1999/11/12 16:57	14.0	7.0

In the case of shallow earthquakes, an iterative procedure (Fukushima *et al.*, 2003) was applied because of the nonlinear term in equation (5). We weighted data in the near-source region to improve the near-source predictive ability of the model. The weighting scheme has no physical meaning but is a useful approach for increasing the statistical power of the near-source data. We used the same weighting scheme as adopted by Midorikawa and Ohtake (2003): 6.0 ($X \leq 25$ km), 3.0 ($25 < X \leq 50$ km), 1.5 ($50 < X \leq 75$ km), and 1.0 ($X > 75$ km).

Kanno et al.(2006)

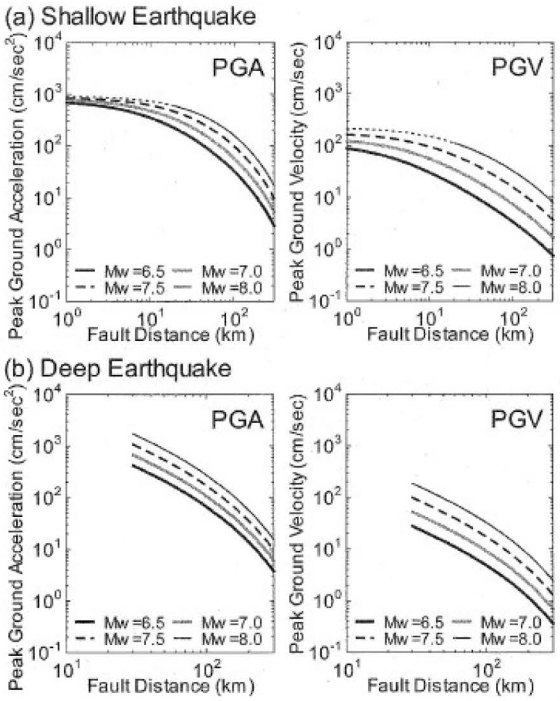

Figure 4. PGV for M earthquake

$$\log \text{pre} = a_1 M_w + b_1 X - \log(X + d_1 \cdot 10^{e_1 M_w}) + c_1 + \varepsilon_1 \quad (D \le 30 \text{ km}) \qquad (5)$$

$$\log \text{pre} = a_2 M_w + b_2 X - \log(X) + c_2 + \varepsilon_2 \quad (D > 30 \text{ km}), \qquad (6)$$

X：断層最短距離

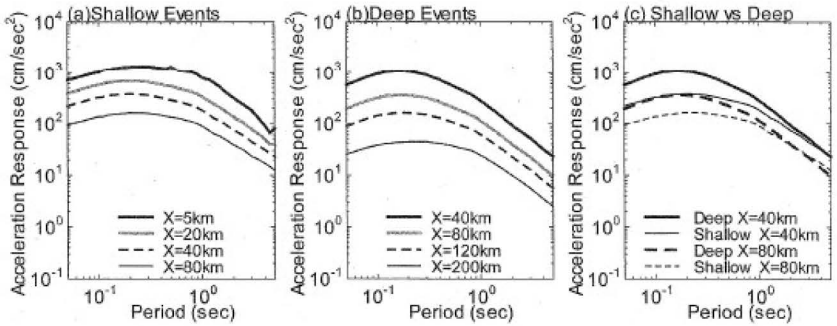

Figure 5. Predicted acceleration response spectra for magnitude 7.0 (a) for shallow and (b) deep events at representative source distances, and (c) a comparison of the response spectra between shallow and deep events at 40 and 80 km source distances.

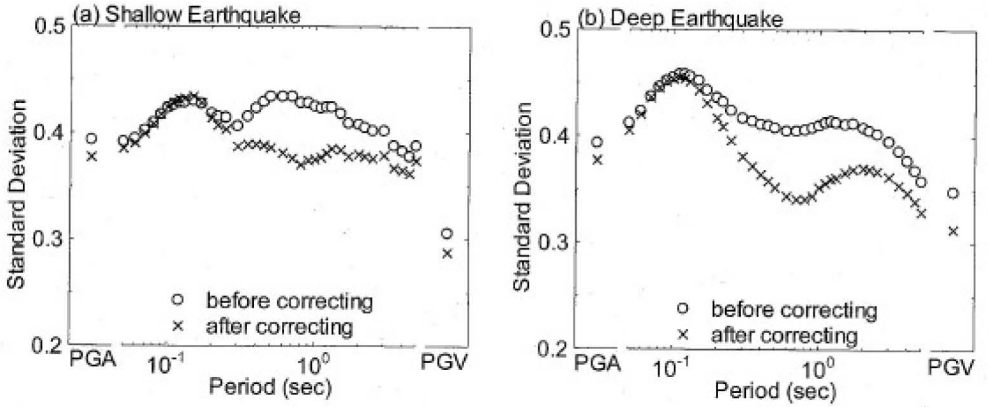

Figure 9. Standard deviations before and after applying the additional correction terms corresponding to site effects: (a) shallow earthquake; (b) deep earthquake.

ばらつき
Standard deviation

Zaho et al.(2006)

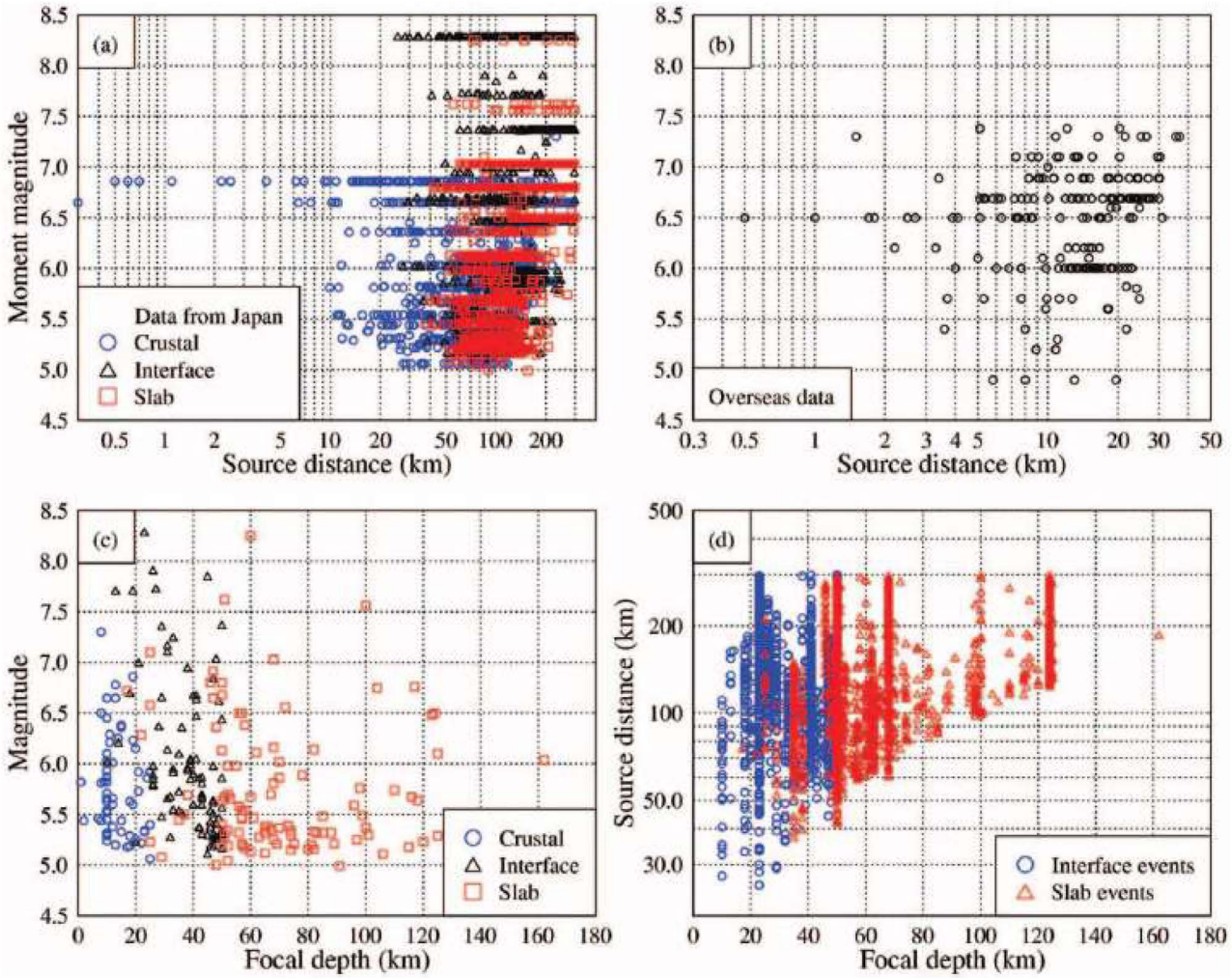

Figure 1. Magnitude-distance distribution for (a) data from Japan; (b) overseas data; (c) magnitude-focal depth distribution; and (d) source distance-focal depth distribution of Japanese data.

Table 1
Numbers of Records by Source Type, Faulting Mechanism, and Region

Focal Mechanism	Crustal	Interface	Slab	Total for Each Focal Mechanism
Japan				
Reverse	250	1492	408	2150
Strike-slip	1011	13	574	1598
Normal	24	3	735	762
Unknown			8	8
Total for each source type	1285	1508	1725	4518
Iran and Western USA				
Reverse	123	12		135
Strike-slip	73			73
Total for each source type	196	12		208
Totals for each source type from all regions				Grand Total
	1481	1520	1725	4726

Table 2
Site Class Definitions Used in the Present Study and the Approximately Corresponding NEHRP Site Classes

Site Class	Description	Natural Period	V_{30} Calculated from Site Period	NEHRP Site Classes
Hard rock			$V_{30} > 1100$	A
SC I	Rock	$T < 0.2$ sec	$V_{30} > 600$	A + B
SC II	Hard soil	$0.2 = T < 0.4$ sec	$300 < V_{30} = 600$	C
SC III	Medium soil	$0.4 = T < 0.6$ sec	$200 < V_{30} = 300$	D
SC IV	Soft soil	$T = 0.6$ sec	$V_{30} = 200$	E + F

Table 3
Numbers of Records by Site Class and Source Type

Source Type	Unknown	SC I	SC II	SC III	SC IV	Total for Each Source Type
Japan						
Crustal	32	427	401	137	288	1285
Interface	9	373	540	186	400	1508
Slab	22	668	530	210	295	1725
Total for each site class	63	1468	1471	533	983	4518
Iran and Western USA						
Crustal		24	73	93	6	196
Interface		2	7	3		12
Total for each site class		26	80	96	6	208
Totals for each site class from all regions						Grand Total
	63	1494	1551	629	989	4726

Zaho et al.(2006)

$$\log_e(y_{i,j}) = aM_{wi} + bx_{i,j} - \log_e(r_{i,j}) + e(h - h_c)\,\delta_h + F_R + S_I + S_S + S_{SL}\log_e(x_{i,j}) + C_k + \xi_{i,j} + \eta_i, \quad (1)$$

$$r_{i,j} = x_{i,j} + c\exp(dM_{wi}), \quad (2)$$

x：断層最短距離

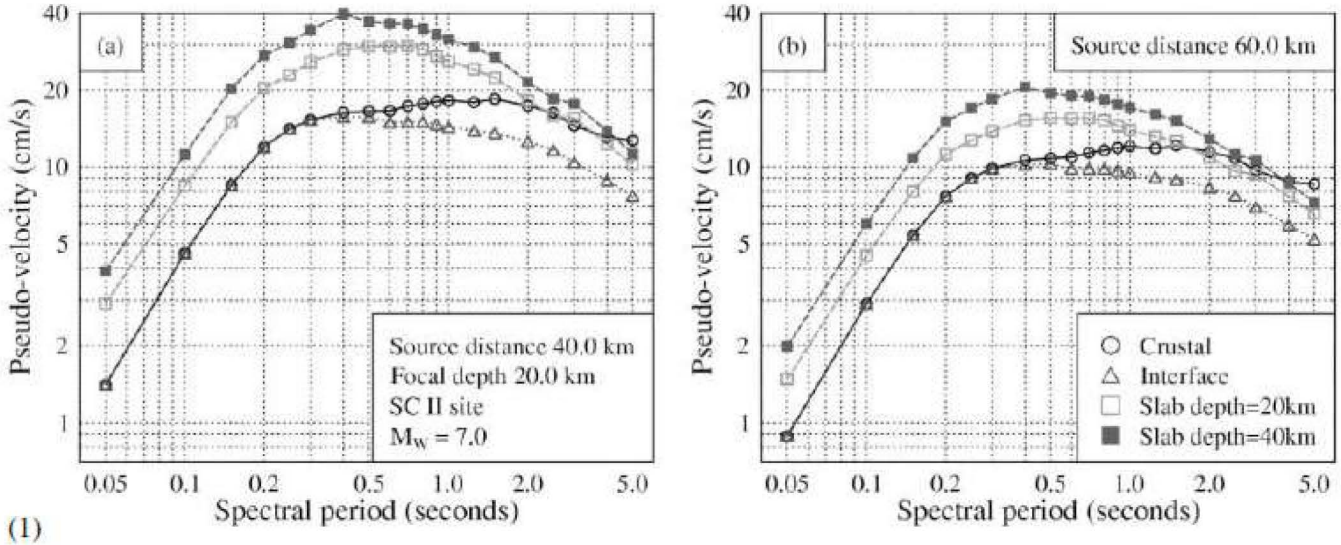

Figure 7. Pseudovelocity spectra calculated for crustal strike-slip and normal events, interface events, and slab events with a magnitude of 7.0 and a depth of 20 km for SC II sites at a source distance of (a) 40 km and (b) 60 km. The spectra from a slab event at a depth of 40 km are also presented for comparison.

ばらつき
Standard deviation

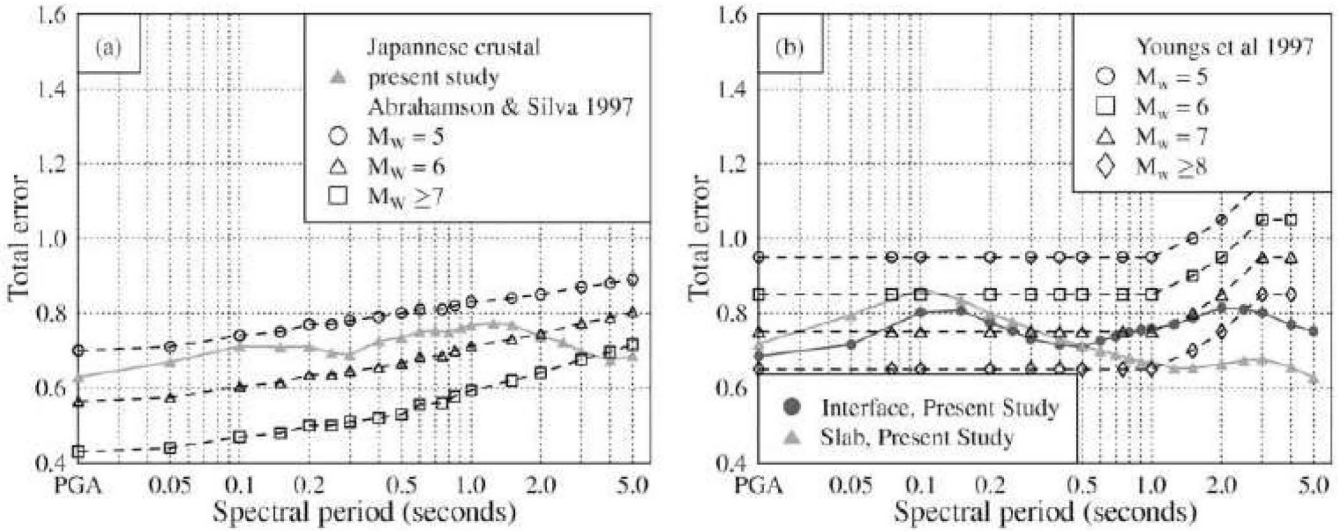

Figure 5. Total standard deviation: (a) crustal events and (b) subduction events.

内山・翠川(2006)

表１　本研究で用いた地震の一覧

No.	地震名	発震日	Mw	Depth (km)	地震タイプ	記録数
1	十勝沖地震	1968.05.16	8.2	15	Inter	8
2	根室半島沖	1973.06.17	7.8	25	Inter	3
3	伊豆大島近海	1978.01.14	6.6	7	Crustal	6
4	宮城県沖	1978.06.12	7.6	37	Inter	7
5	伊豆半島東方沖	1980.06.29	6.5	7	Crustal	10
6	浦河沖	1982.03.21	6.9	25	Crustal	9
7	日本海中部	1983.05.26	7.8	6	Inter	13
8	日向灘	1984.08.07	6.9	30	Intra	3
9	日高山脈北部	1987.01.14	6.8	120	Intra	4
10	千葉県東方沖	1987.12.17	6.7	30	Intra	46
11	釧路沖	1993.01.15	7.6	105	Intra	13
12	能登半島沖	1993.02.07	6.3	15	Crustal	5
13	北海道南西沖	1993.07.12	7.7	10	Inter	14
14	北海道東方沖	1994.10.04	8.3	35	Intra	15
15	三陸はるか沖	1994.12.28	7.7	35	Inter	13
16	兵庫県南部	1995.01.17	6.9	10	Crustal	36
17	日向灘	1996.10.19	6.7	25	Inter	103
18	鹿児島県北西部	1997.03.26	6.1	6	Crustal	101
19	鹿児島県北西部	1997.05.13	6.0	7	Crustal	100
20	山口県北部	1997.06.25	5.8	10	Crustal	119
21	伊豆半島東方沖	1998.05.03	5.5	3	Crustal	76
22	岩手県内陸北部	1998.09.03	5.8	10	Crustal	55
23	日向灘	1998.12.16	5.8	32	Inter	43
24	釧路支庁中南部	1999.05.13	6.4	104	Intra	70
25	和歌山県北部	1999.08.21	5.8	70	Intra	114
26	根室半島南東沖	2000.01.28	6.7	56	Intra	30
27	千葉県北東部	2000.06.03	5.9	48	Inter	104
28	茨城県沖	2000.07.21	6.1	49	Inter	108
29	鳥取県西部	2000.10.06	6.8	11	Crustal	179
30	三重県南部	2000.10.31	5.5	43	Intra	133
31	芸予	2001.03.24	6.7	51	Intra	193
32	日向灘	2001.04.25	5.6	42	Intra	99
33	根室半島南東沖	2001.04.27	6.0	83	Intra	32
34	青森県東方沖	2001.08.14	6.4	43	Inter	71
35	岩手県内陸南部	2001.12.02	6.5	122	Intra	93
36	北海道東方沖	2002.01.19	5.7	32	Intra	10
37	茨城県沖	2002.02.12	5.5	48	Inter	112
38	福島県沖	2002.07.24	5.5	30	Inter	39
39	北海道東方沖	2002.07.25	5.7	12	Inter	11
40	根室半島南東沖	2002.08.25	6.1	44	Inter	30
41	福島県沖	2002.10.12	5.5	29	Inter	21
42	青森県東方沖	2002.10.14	6.0	53	Inter	71
43	宮城県沖	2002.11.03	6.4	46	Inter	57
44	日向灘	2002.11.04	5.7	35	Intra	90
45	福島県沖	2003.03.03	5.7	41	Inter	57
46	北海道東方沖	2003.04.29	5.9	18	Inter	5
47	宮城県沖	2003.05.26	7.0	71	Intra	132
48	釧路沖	2003.07.03	5.8	33	Inter	41
49	宮城県北部	2003.07.26	5.5	12	Crustal	82
50	宮城県北部	2003.07.26	6.1	12	Crustal	97
51	千葉県東方沖	2003.09.20	5.7	70	Inter	115
52	十勝沖	2003.09.26	7.9	42	Inter	200

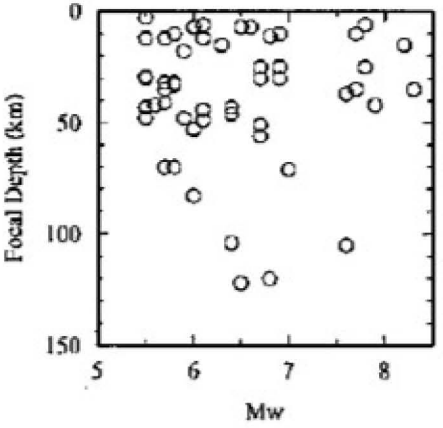

図１　Mwと震源深さの分布

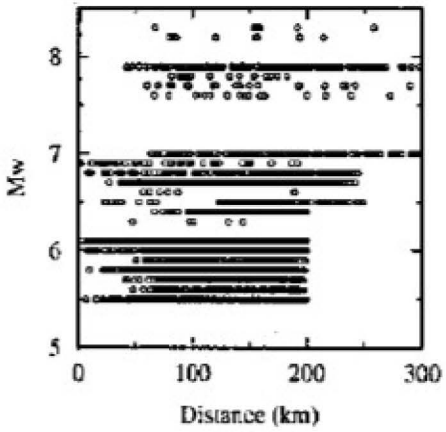

図３　断層面最短距離とMwの分布

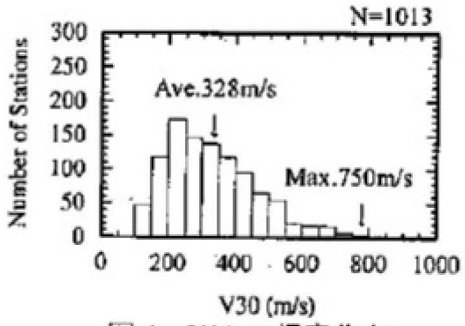

図４　V30の頻度分布

表２　V30に基づく地盤分類

地盤分類	V30 (m/s)
A	V30>1500
B	760<V30≦1500
C1	460<V30≦760
C2	360<V30≦460
D1	250<V30≦360
D2	180<V30≦250
E	V30≦180

内山・翠川(2006)

$$\log SA(T) = a(T)M_w + b(T)X + g + d(T)D + c(T) + \sigma(T) \quad (8)$$

$$\log SA(T) = a(T)M_w + b(T)X + g + d(T)D + \sum_{i=1}^{2} f_i(T)F_i + c(T) + \sigma(T) \quad (9)$$

X：断層最短距離

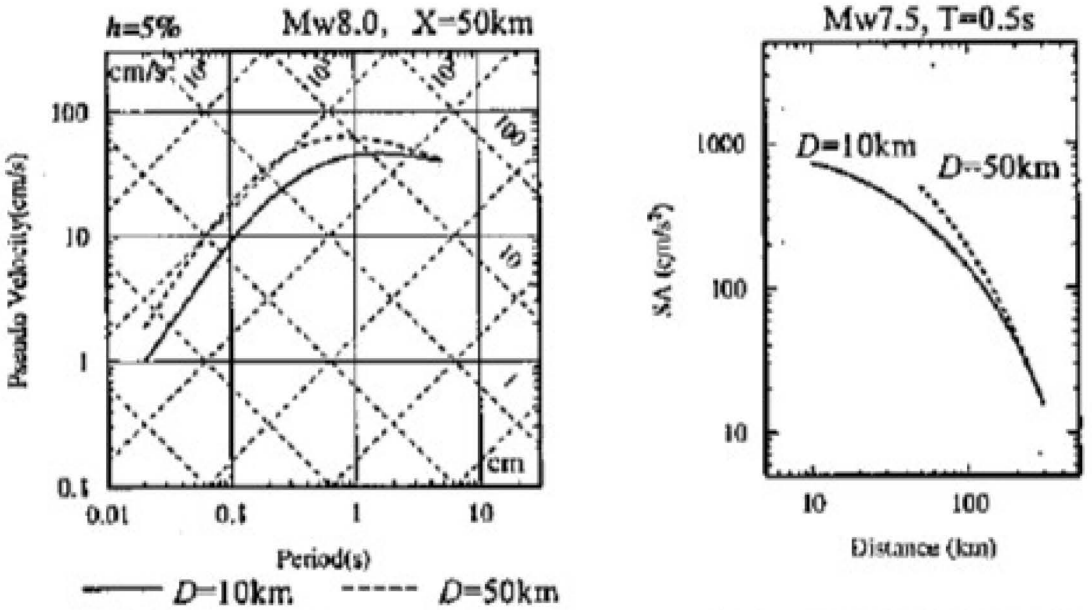

(a) 応答スペクトルの比較　　(b) 距離減衰の比較

図 15 震源深さが予測値に与える影響

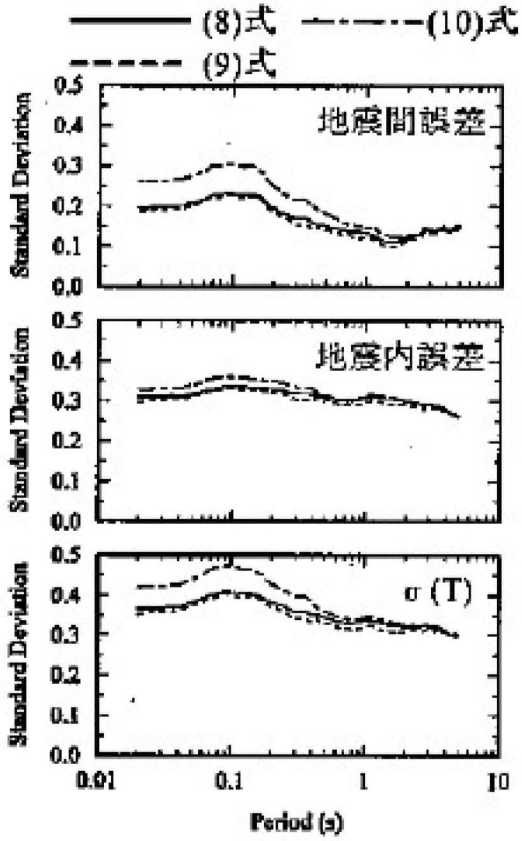

図 8 回帰誤差の比較

ばらつき
Standard deviation

片岡・ほか(2006)

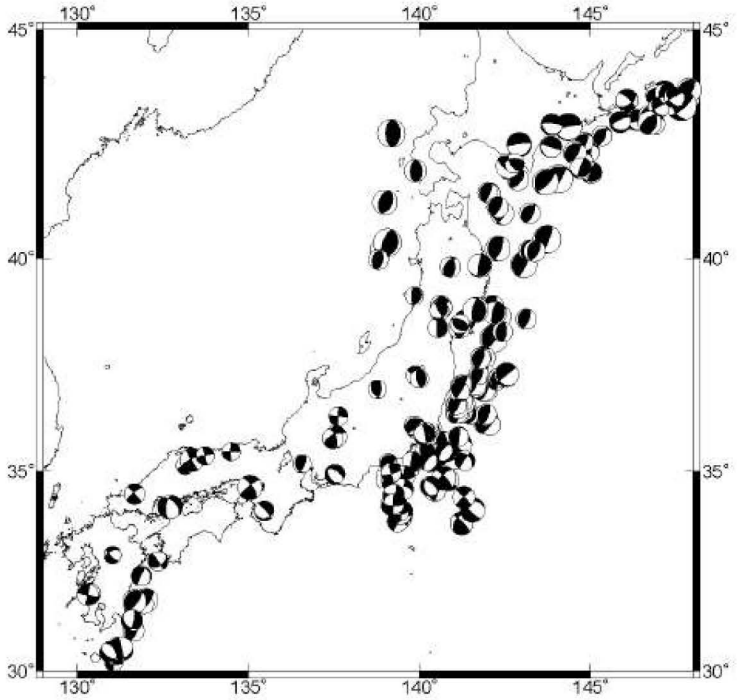

図-1　距離減衰式の作成に用いた全地震（1978 年 6 月～2003 年 9 月）の震央位置とメカニズム解

表-1　距離減衰式の作成に用いた地震，観測点，波形の数

	内陸地震	海溝性地震
地震数	47	136
観測点数	961	1050
波形数	5160	5882

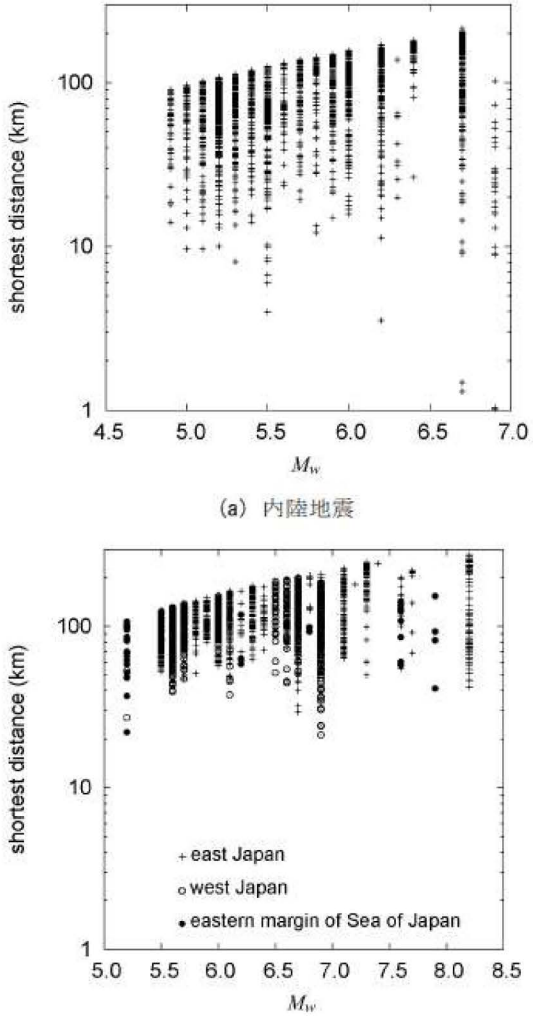

図-2　強震記録が得られた地震のモーメントマグニチュード M_w と断層面最短距離との関係

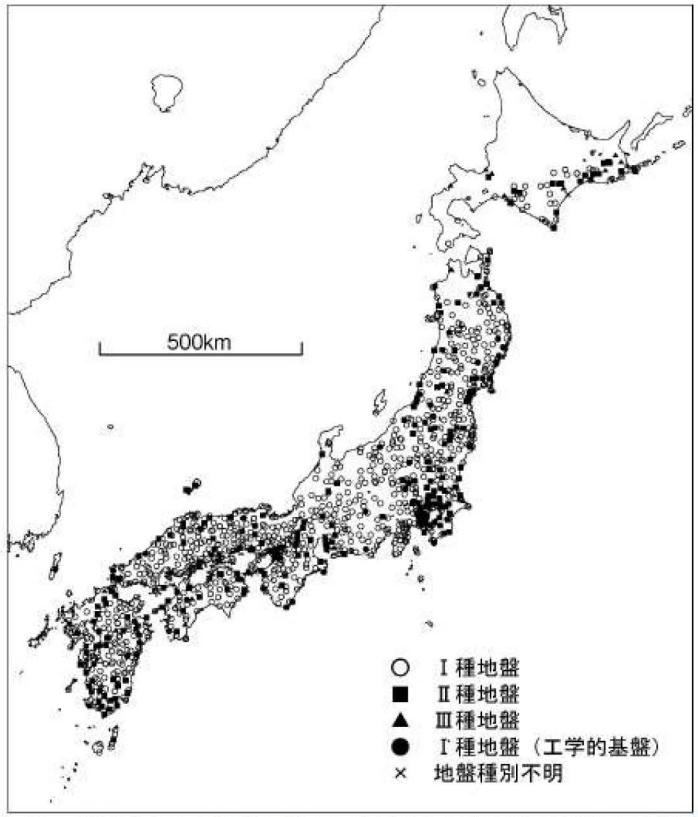

図-3　距離減衰式の作成に用いた強震記録が得られた観測点の位置

片岡・ほか(2006)

$$\log_{10} Y_{ij} = a_1 M_w + a_2 \log_{10} A - bX + c_0 - \log_{10}(X + d \cdot 10^{0.5M_w}) + c_j \pm e \quad (29)$$

A：短周期レベル

$$\log_{10} Y_{ij} = a_1 M_w + a_2 D - bX + c_0 - \log_{10}(X + d \cdot 10^{0.5M_w}) + c_j \pm e \quad (30)$$

D：震源深さ

$$\log_{10} Y_{ij} = a_1 M_w - bX + c_0 - \log_{10}(X + d \cdot 10^{0.5M_w}) + c_j \pm e \quad (31)$$

X：断層最短距離

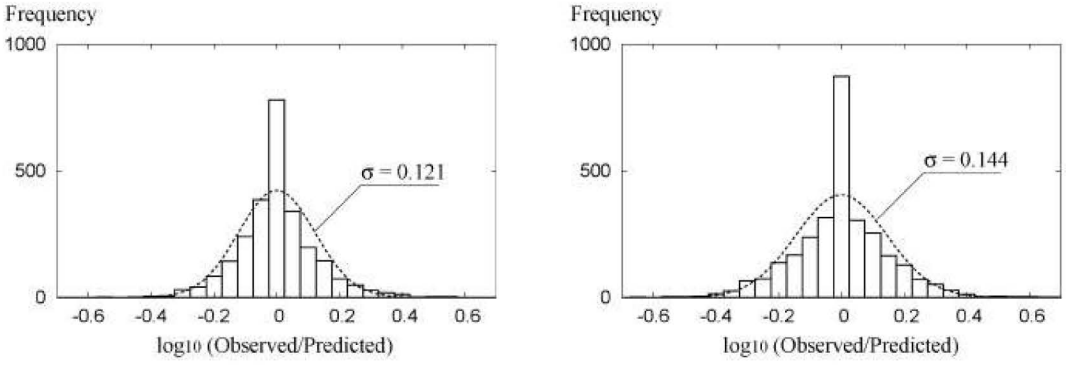

(a) 内陸地震の *PGV*　(b) 海溝性地震の *PGV*

図-8　距離減衰式の地震内誤差

ばらつき
Standard deviation

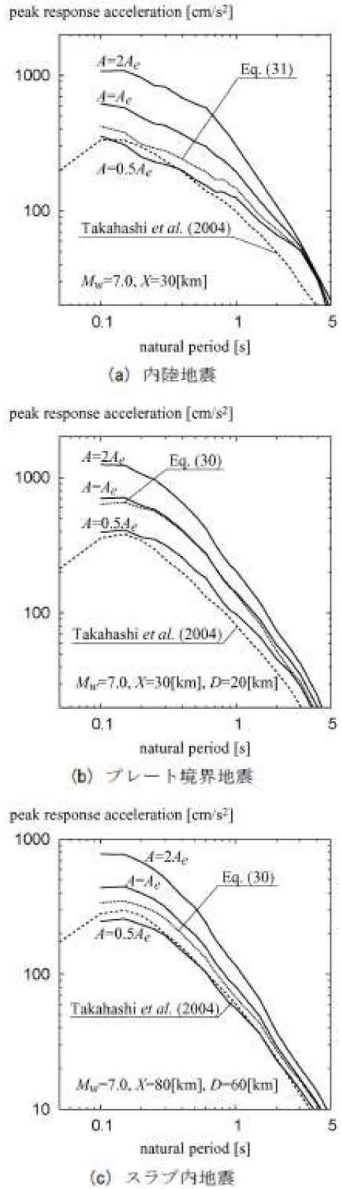

図-11　距離減衰式により推定される加速度応答スペクトル（工学的基盤）の比較

Si et al.(2013)

Table 1 Earthquakes used in this study

EQ. No.	EQ. NAME	Initial Date	Time	Mw	Depth	Fault Type	Number of Data
1	Nihon-kai Chubu	1983.05.26	11:59	7.8	6.0	Inter	3
2	Eastern Off Chiba	1987.12.17	11:08	6.7	30.0	Intra	10
3	Off Kushiro	1993.01.15	20:06	7.6	105.0	Intra	8
4	Off Noto-hanto	1993.02.07	22:27	6.3	15.0	Crustal	3
5	Hokkaido-Nansei-Oki	1993.07.12	22:17	7.7	10.0	Inter	4
6	Hokkaido-Toho-Oki	1994.10.04	22:22	8.3	35.0	Intra	5
7	Sanriku-Haruka-Oki	1994.12.28	21:19	7.7	35.0	Inter	11
8	Hyogo-ken Nanbu	1995.01.17	5:46	6.9	10.0	Crustal	34
9	North-Western Kagoshima	1997.03.26	17:31	6.1	6.0	Crustal	3
10	North-Western Kagoshima	1997.05.13	14:38	6.0	7.0	Crustal	3
11	Izu Hanto Toho-Oki	1998.05.03	11:09	5.6	3.0	Crustal	8
12	Western Tottori	2000.10.06	13:30	6.8	11.0	Crustal	50
13	Geiyo	2001.03.24	15:27	6.7	51.0	Intra	40
14	Miyagi-ken Oki	2002.11.03	12:37	6.4	46.0	Inter	21
15	Hyuganada	2002.11.04	13:36	5.6	35.0	Intra	9
16	Miyagi-ken Oki	2003.05.26	18:24	7.0	71.0	Intra	33
17	Northern Miyagi	2003.07.26	7:13	6.1	12.0	Crustal	9
18	Tokachi Oki	2003.09.26	4:50	8.3	35.0	Inter	16
19	Chuetsu	2004.10.23	17:56	6.6	10.0	Crustal	30
20	Kushiro-oki	2004.11.29	3:32	7.0	48.0	Inter	5
21	Western Fukuoka	2005:03:20	10:53	6.6	9.0	Crustal	25
22	Miyagi-ken Oki	2005.08.16	11:46	7.1	42.0	Inter	42
23	Chuetsu-oki	2007.07.16	10:13	6.6	10.0	Crustal	22
24	Ibaraki-oki	2008.05.08	1:45	6.8	51.0	Inter	11
25	Iwate-Miyagi Nairiku	2008.06.14	8:43	6.9	10.0	Crustal	30
26	Northern Iwate	2008.07.24	0:26	6.8	108.0	Intra	24
27	Surugawa	2009.08.11	5:07	6.2	23.0	intra	30
28	Tohoku	2011.03.11	14:46	9.1	25.0	Inter	34
29	Off-Iwate	2011.03.11	15:08	7.4	32.0	Inter	10
30	Off-Ibaraki	2011.03.11	15:15	7.9	38.0	Inter	20
31	Norther Nagano	2011.03.12	3:59	6.3	7.0	Crustal	15
32	Eastern Shizuoka	2011.03.15	22:31	6.0	10.0	Crustal	13
33	Off Miyagi	2011.04.07	23:32	7.1	59.0	Intra	35
34	Hama-dori	2011.04.11	17:16	6.7	10.0	Crustal	20

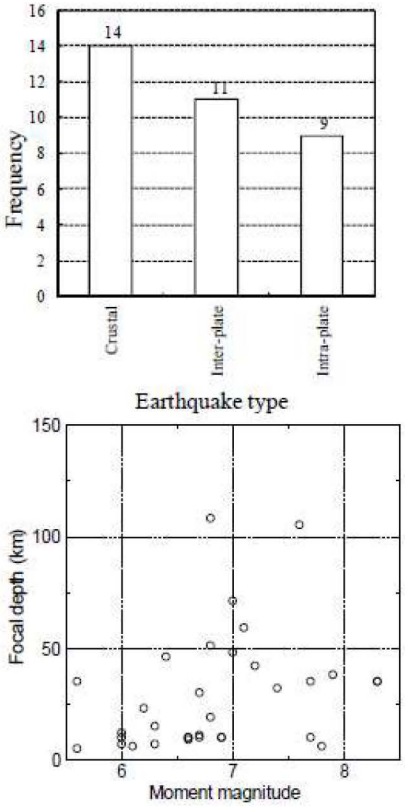

Figure 1 histogram of the earthquake type (upper) and the plot of moment magnitude vs. the focal depth (lower)

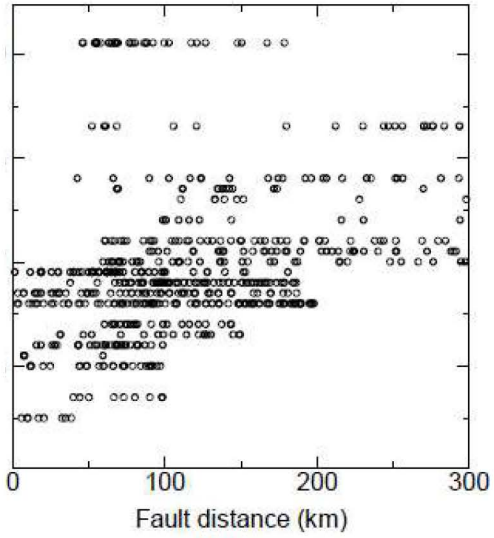

ıre 2 Distribution of Mw vs. fault distance

Si et al.(2013)

$$\log SA(T) = b(T) + g(X) - kX + \varepsilon(T)$$

$$g(X) = \begin{cases} -\log(X + C); D \le 30km \\ 0.6\log(1.7D + C) - 1.6\log(X + C); D > 30km \ \& \ X \ge 1.7D \end{cases}$$

X：断層最短距離

$$C = 0.0055 \cdot 10^{0.5M_w}, T < 0.3s$$

$$= 0.0028 \cdot 10^{0.5M_w}, T \ge 0.6s$$

$$k = 0.003, T < 0.3s$$

$$= 0.002, T \ge 0.6s$$

(1)

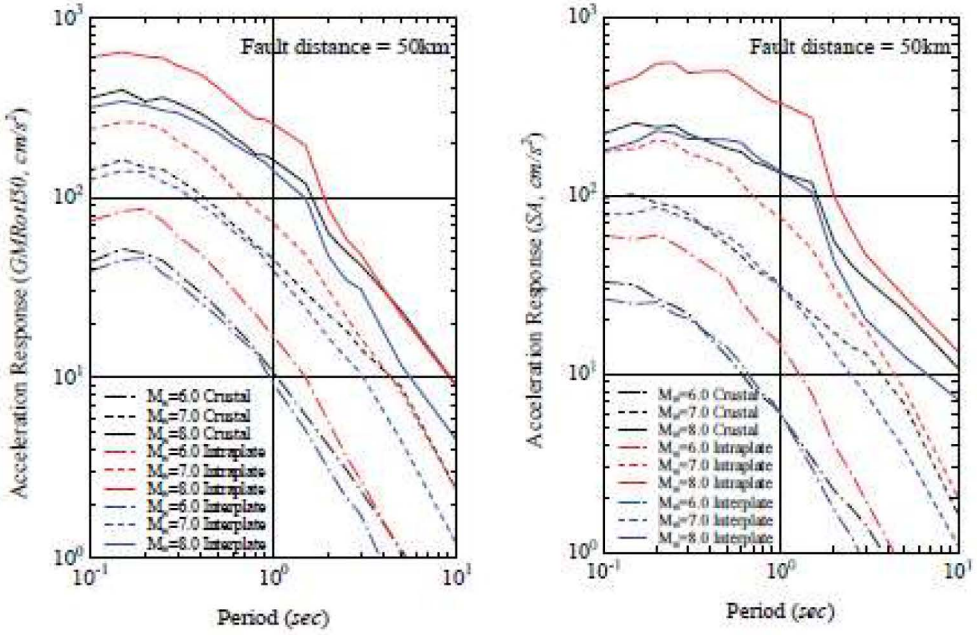

Figure 7 Predicted response spectra based on the results (Left: horizontal component; Right: vertical component)

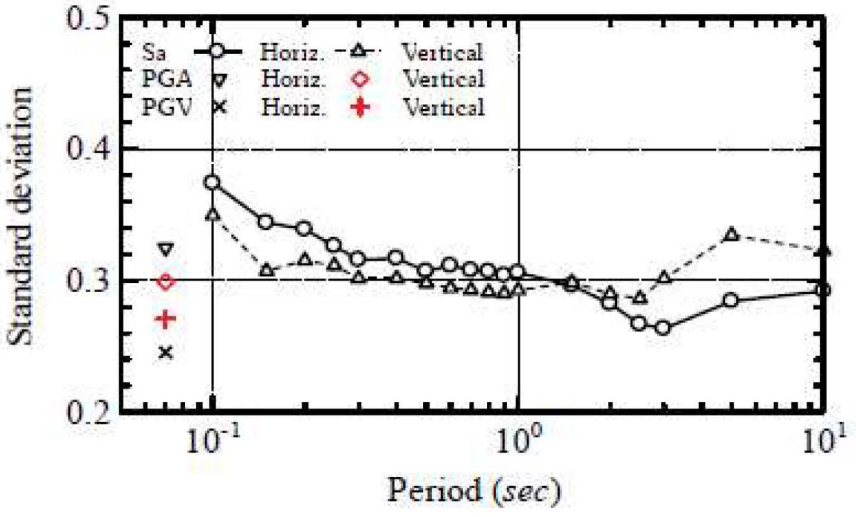

Figure 9 Standard deviation for the GMPE proposed in this study.

ばらつき
Standard deviation

Database of NGA-West2

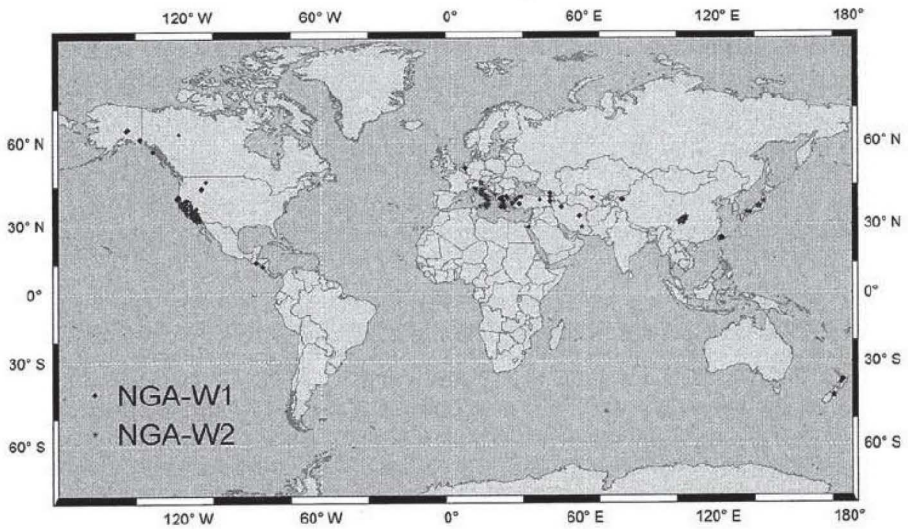

Figure 1. Epicenter distribution of 599 events included in the NGA-West2 database.

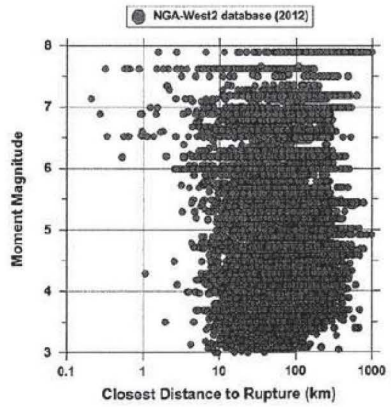

Figure 1. Distribution of recordings of the 1997 PEER, NGA-West1 and NGA-West2 ground motion databases with magnitude and distance.

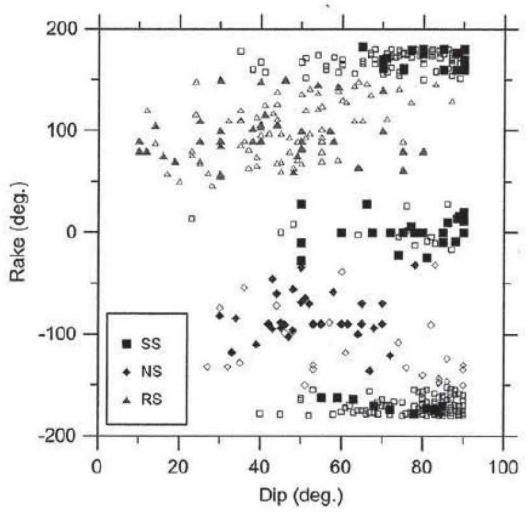

Figure 5. Rake versus dip scatter plot for events in the NGA-West2 database. Open symbols represent events that were added, solid symbols represent events in the NGA-West1 database. The three predominant mechanisms (strike slip, or SS; normal slip, or NS; and reverse slip, or RS) are illustrated as indicated by legend, based on rake angle assignments in the flatfile (AEA13). These boundaries are for illustrative purposes and are not universally applied.

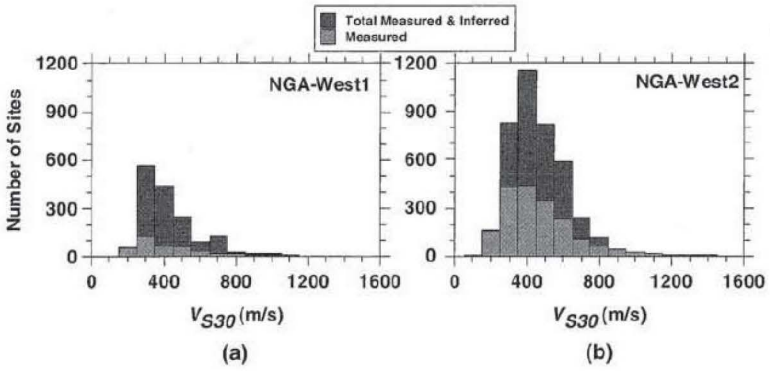

Figure 2. Distribution of V_{S30} in (a) NGA-West1 and (b) NGA-West2 databases (adapted from Seyhan and Stewart 2014). A site is considered as "measured" if there is a measured shear-wave velocity in the top 10 m (or deeper) of soil or rock.

NGA-West2

- Definition of parameters

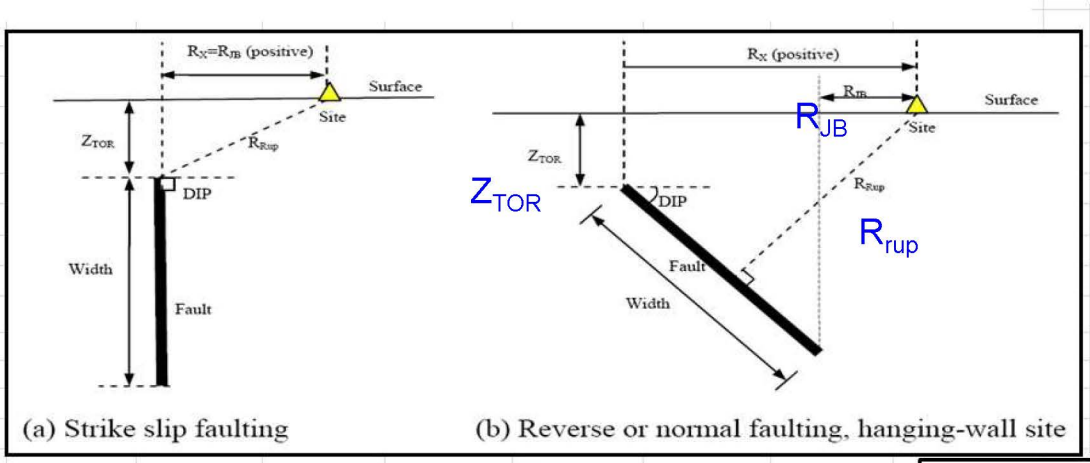

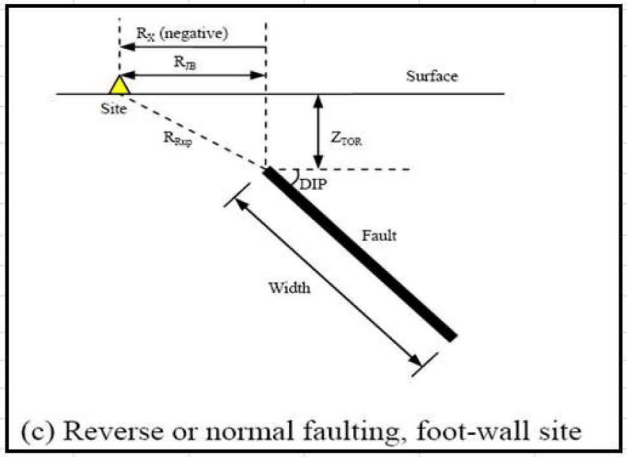

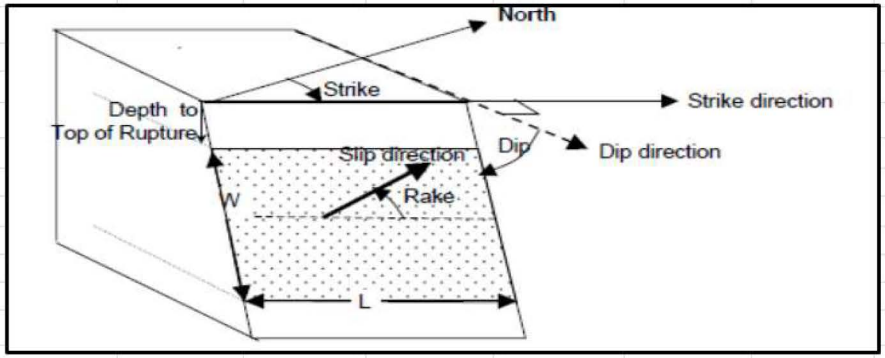

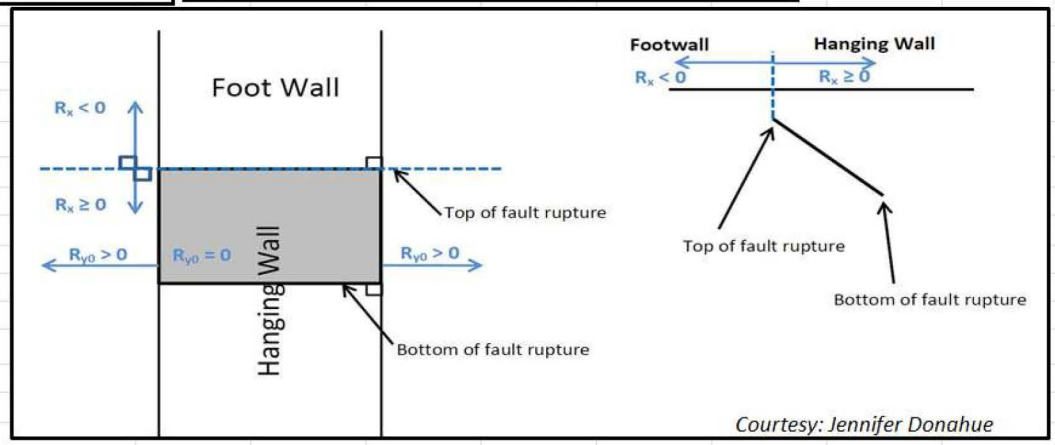

Abrahamson et al.(2014)

断層種別　　本震/余震の別

$$\ln Sa(g) = f_1(\mathbf{M}, R_{RUP}) + F_{RV} f_7(\mathbf{M}) + F_N f_8(\mathbf{M}) + F_{As} f_{11}(CR_{JB})$$

サイト特性（浅部地盤）　　上盤効果

$$+ f_5(\widehat{Sa}_{1180}, V_{S30}) + F_{HW} f_4(R_{JB}, R_{RUP}, R_x, R_{y0}, W, dip, Z_{TOR}, \mathbf{M})$$

$$+ f_6(Z_{TOR}) + f_{10}(Z_1, V_{S30}) + Regional(V_{S30}, R_{RUP}) \qquad (1)$$

断層上端深さ　　深部地盤特性　　地域補正（米国/日本/中国/台湾）

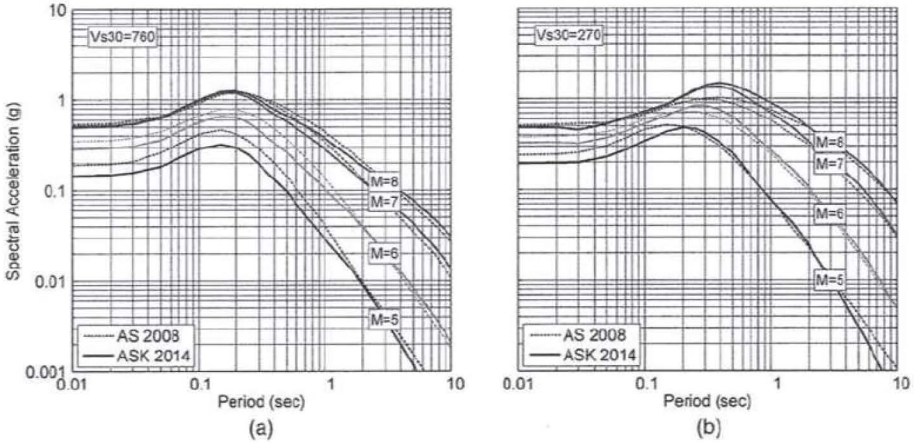

Figure 7. Comparison of the median spectral acceleration from the current model with the median from the AS08 model for vertical strike-slip earthquakes for $R_{JB} = 1$ km. (a) $V_{S30} = 760$ m/s, (b) $V_{S30} = 270$ m/s.

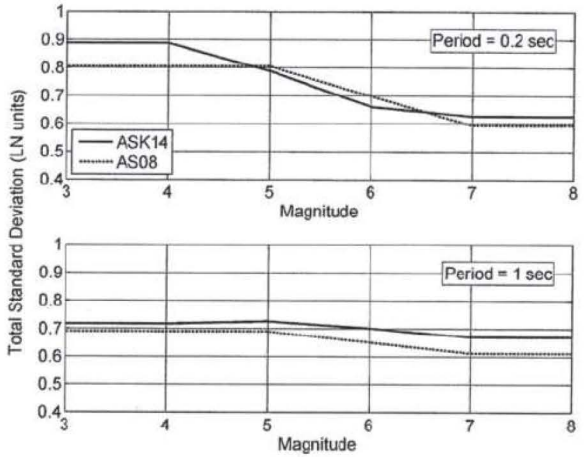

Figure 16. Magnitude dependence of the total standard deviation for a strike-slip event at $R_{RUP} = 30$ km and a measured $V_{S30} = 760$ m/s. Comparison between ASK14 and AS08 for $T = 0.2$ s and $T = 1.0$ s.

ばらつき
Standard deviation

Boore et al.(2014)

震源　減衰　サイト

$$\ln Y = F_E(\mathbf{M}, mech) + F_P(R_{JB}, \mathbf{M}, region) + F_S(V_{S30}, R_{JB}, \mathbf{M}, region, z_1) + \varepsilon_n \sigma(\mathbf{M}, R_{JB}, V_{S30}) \quad (1)$$

標準偏差　震源タイプ

$$F_E(\mathbf{M}, mech) = \begin{cases} e_0 U + e_1 SS + e_2 NS + e_3 RS + e_4(\mathbf{M} - \mathbf{M}_h) + e_5(\mathbf{M} - \mathbf{M}_h)^2 & \mathbf{M} \le \mathbf{M}_h \\ e_0 U + e_1 SS + e_2 NS + e_3 RS + e_6(\mathbf{M} - \mathbf{M}_h) & \mathbf{M} > \mathbf{M}_h \end{cases} \quad (2)$$

$$F_P(R_{JB}, \mathbf{M}, region) = [c_1 + c_2(\mathbf{M} - \mathbf{M}_{ref})] \ln(R/R_{ref}) + (c_3 + \Delta c_3)(R - R_{ref}) \quad (3)$$

幾何減衰　非弾性減衰、ΔC3は地域項（国）

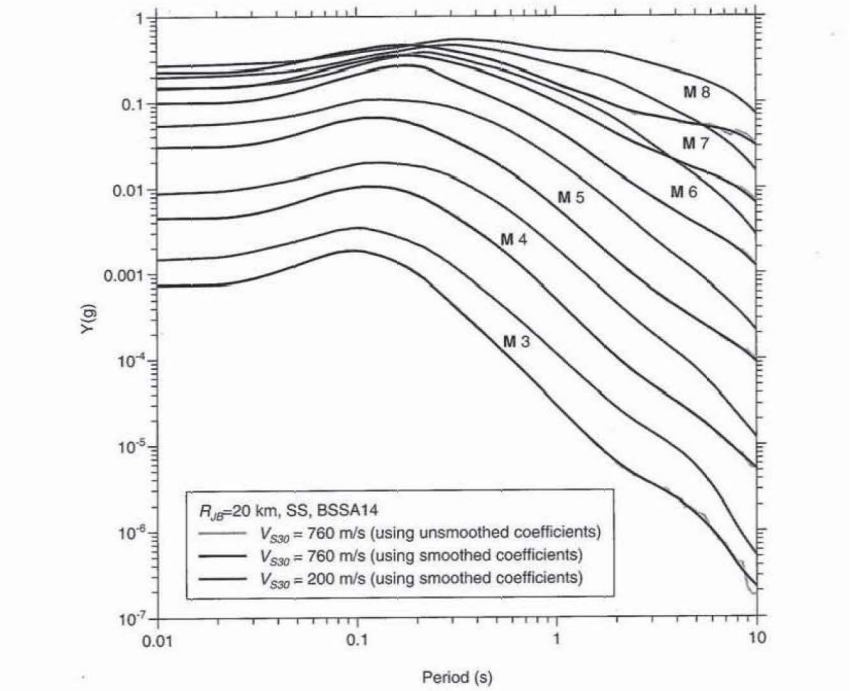

Figure 8. Variation of median predicted PSA versus period (T) for **M** 3, 4, 5, 6, 7, and 8 strike-slip earthquakes for R_{JB} = 20 km and V_{S30} = 200 m/s and 760 m/s.

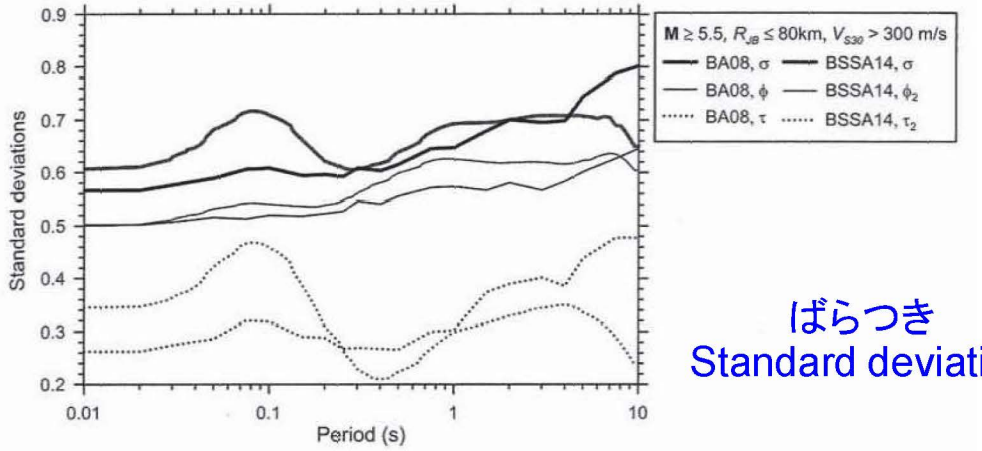

ばらつき
Standard deviation

Figure 16. Comparison of the standard deviation terms in the BSSA14 GMPEs for **M** ≥ 5.5, R_{JB} < 80 km and V_{S30} > 300 m/s with the **M**- and R_{JB}-independent standard deviations from BA08.

$$\sigma(\mathbf{M}, R_{JB}, V_{S30}) = \sqrt{\phi^2(\mathbf{M}, R_{JB}, V_{S30}) + \tau^2(\mathbf{M})}$$

地震内誤差　地震間誤差

Cambelle and Bozorgnia(2014)

$$\ln Y = \begin{cases} \ln PGA; & PSA < PGA \text{ and } T < 0.25 \text{ s} \\ f_{mag} + f_{dis} + f_{flt} + f_{hng} + f_{site} + f_{sed} + f_{hyp} + f_{dip} + f_{atn}; & \text{otherwise} \end{cases}$$

震源 幾何減衰 上盤効果 盆地 傾斜角

断層タイプ 浅部地盤 震源深さ 減衰

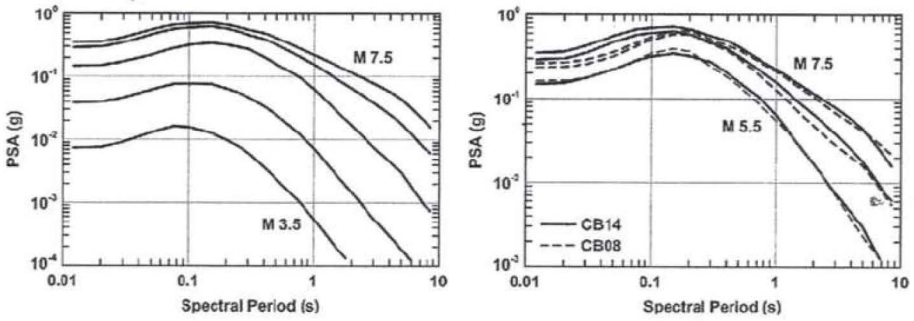

Figure 9. Median estimates of CB14 response spectra for $R_{RUP} = 10$ km and for $\mathbf{M} = 3.5$, 4.5, 5.5, 6.5 and 7.5 (left panel) as compared to median estimates of CB08 response spectra for $\mathbf{M} = 5.5$, 6.5 and 7.5 (right panel) where both GMPEs are considered to be valid. All other predictor variables are evaluated as indicated in the caption to Figure 6.

ばらつき Standard deviation

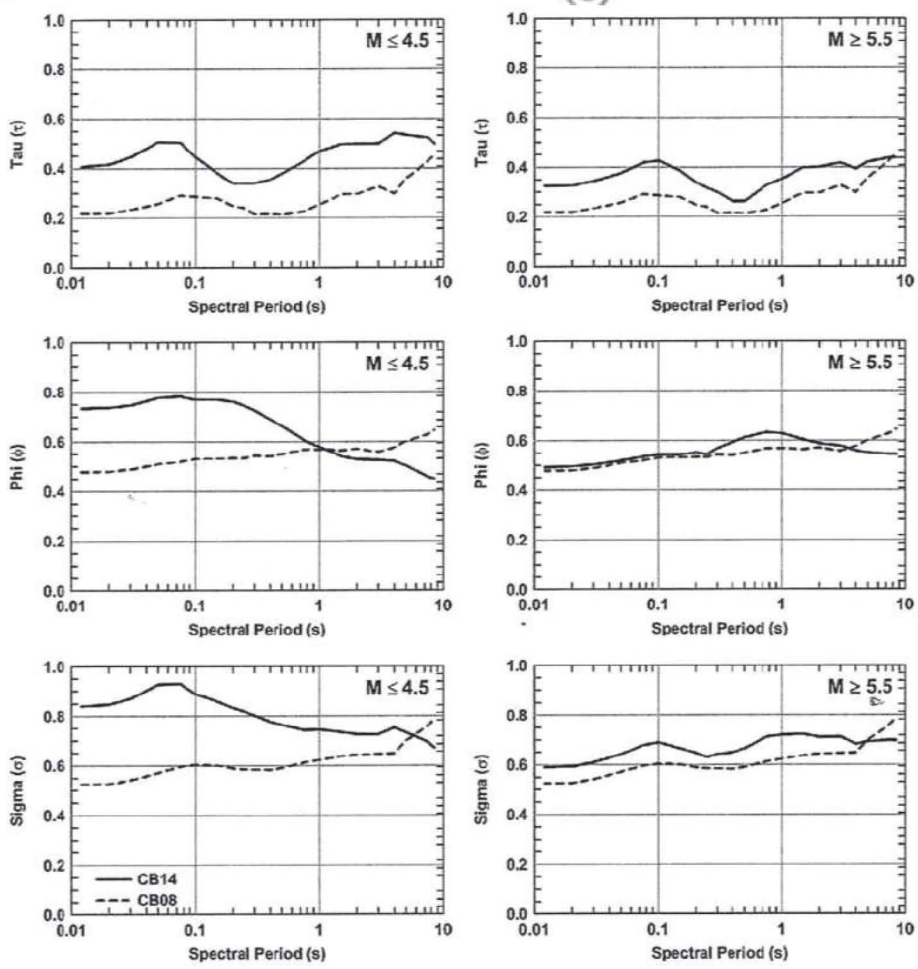

Figure 11. Comparison of CB14 and CB08 linear between-event (τ), within-event (ϕ), and total (σ) standard deviations for small ($\mathbf{M} \leq 4.5$) and moderate-to-large ($\mathbf{M} \geq 4.5$) magnitudes. Standard deviations between these two magnitude limits are calculated by linear interpolation.

Chiou and Youngs(2014)

$$
\begin{aligned}
\ln(y_{refij}) = {} & c_1 + \left\{c_{1a} + \frac{c_{1c}}{\cosh(2 \cdot \max(\mathbf{M}_i - 4.5, 0))}\right\} F_{RVi} && \text{逆断層} \\
& + \left\{c_{1b} + \frac{c_{1d}}{\cosh(2 \cdot \max(\mathbf{M}_i - 4.5, 0))}\right\} F_{NMi} && \text{正断層} \\
& + \left\{c_7 + \frac{c_{7b}}{\cosh(2 \cdot \max(\mathbf{M}_i - 4.5, 0))}\right\} \Delta Z_{TORi} && \text{上端深さ} \\
& + \left\{c_{11} + \frac{c_{11b}}{\cosh(2 \cdot \max(\mathbf{M}_i - 4.5, 0))}\right\} (\cos \delta_i)^2 && \text{傾斜角} \\
& + c_2(\mathbf{M}_i - 6) + \frac{c_2 - c_3}{c_n} \ln(1 + e^{c_n(c_M - \mathbf{M}_i)}) && \text{地震規模} \\
& + c_4 \ln(R_{RUPij} + c_5 \cosh(c_6 \cdot \max(\mathbf{M}_i - c_{HM}, 0))) \\
& + (c_{4a} - c_4) \ln\left(\sqrt{R_{RUPij}^2 + c_{RB}^2}\right) && \text{距離減衰} \\
& + \left\{c_{\gamma 1} + \frac{c_{\gamma 2}}{\cosh(\max(\mathbf{M}_i - c_{\gamma 3}, 0))}\right\} R_{RUPij} \\
& + c_8 \max\left(1 - \frac{\max(R_{RUPij} - 40, 0)}{30}, 0\right) \\
& \times \min\left(\frac{\max(\mathbf{M}_i - 5.5, 0)}{0.8}, 1\right) e^{-c_{8a}(\mathbf{M}_i - c_{8b})^2} \Delta DPP_{ij} && \text{破壊伝播効果} \\
& + c_9 F_{HWij} \cos \delta_i \left\{c_{9a} + (1 - c_{9a}) \tanh\left(\frac{R_{Xij}}{c_{9b}}\right)\right\} \left\{1 - \frac{\sqrt{R_{JBij}^2 + Z_{TORi}^2}}{R_{RUPij} + 1}\right\} && \text{上盤効果}
\end{aligned} \tag{11}
$$

$$
\begin{aligned}
\ln(y_{ij}) = {} & \ln(y_{ref_{ij}}) + \eta_i \\
& + \phi_1 \cdot \min\left(\ln\left(\frac{V_{S30j}}{1130}\right), 0\right) \\
& + \phi_2 \left(e^{\phi_3(\min(V_{S30j}, 1130) - 360)} - e^{\phi_3(1130 - 360)}\right) \ln\left(\frac{y_{ref_{ij}} e^{\eta_i} + \phi_4}{\phi_4}\right) \\
& + \phi_5 (1 - e^{-\Delta Z_{1.0j}/\phi_6}) \\
& + \varepsilon_{ij}
\end{aligned} \tag{12}
$$

地盤増幅の考慮

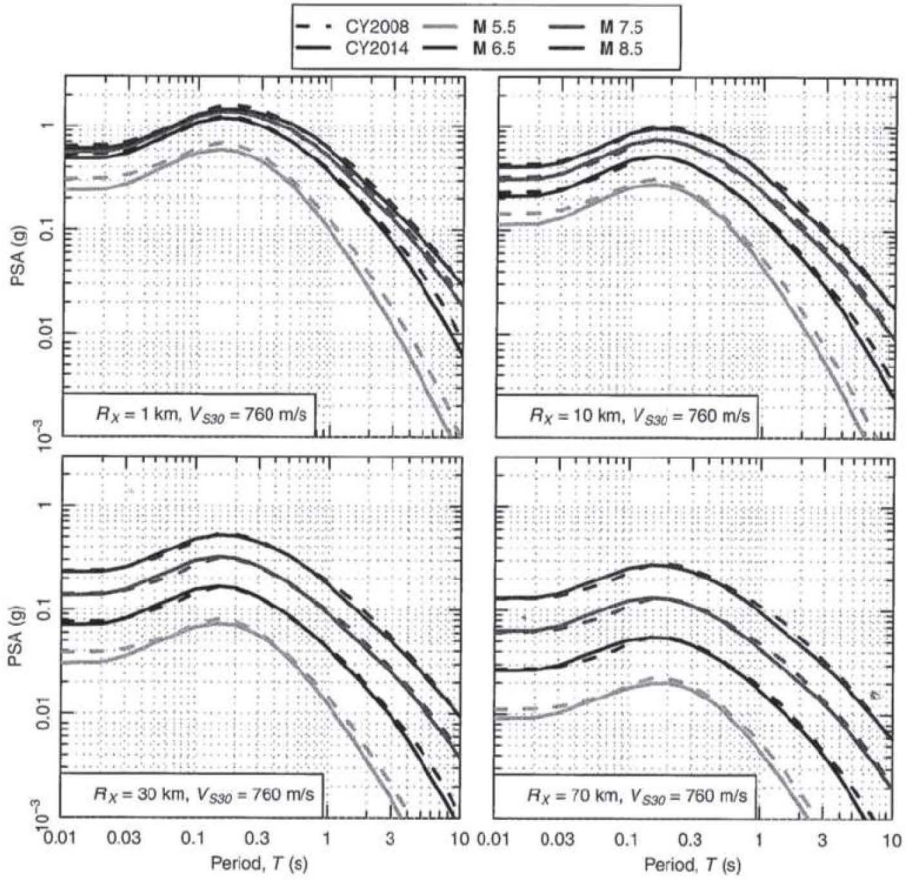

Figure 16. Median response spectra predicted by the 2008 Chiou and Youngs NGA model (CY2008) and the updated model (CY2014). Predictions are for vertical strike-slip earthquakes and $V_{S30} = 760$ m/s.

Idriss(2014)

$$Ln[PSA] = \alpha_1 + \alpha_2 \mathbf{M} + \alpha_3 (8.5 - \mathbf{M})^2 - [\beta_1 + \beta_2 \mathbf{M}] Ln(R_{RUP} + 10) + \xi Ln(V_{S30}) + \gamma R_{RUP} + \varphi F$$

メカニズム項

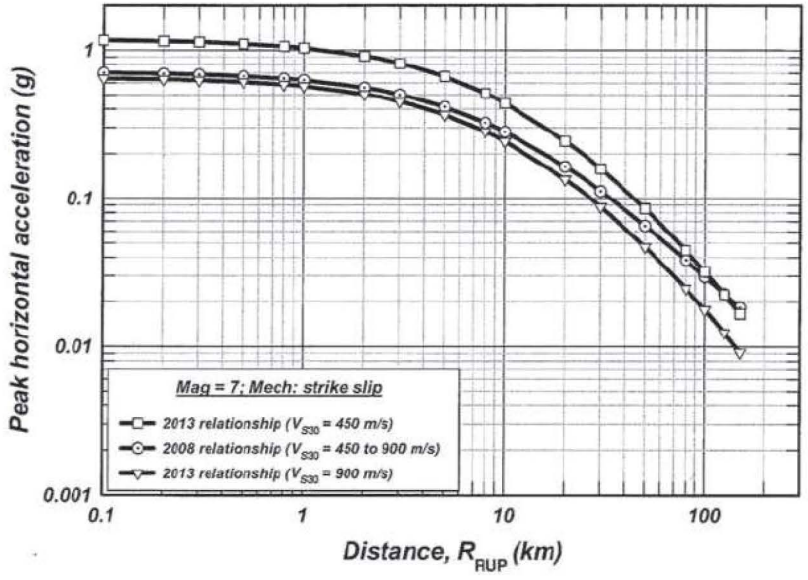

Figure 15. PGA versus R_{RUP} for $\mathbf{M} = 7$ occurring on a strike-slip source calculated using th coefficients derived for the 2008 model (V_{S30} = 450 to 900 m/s) and the coefficients derived fo the 2013 model for V_{S30} = 450 m/s and for V_{S30} = 900 m/s.

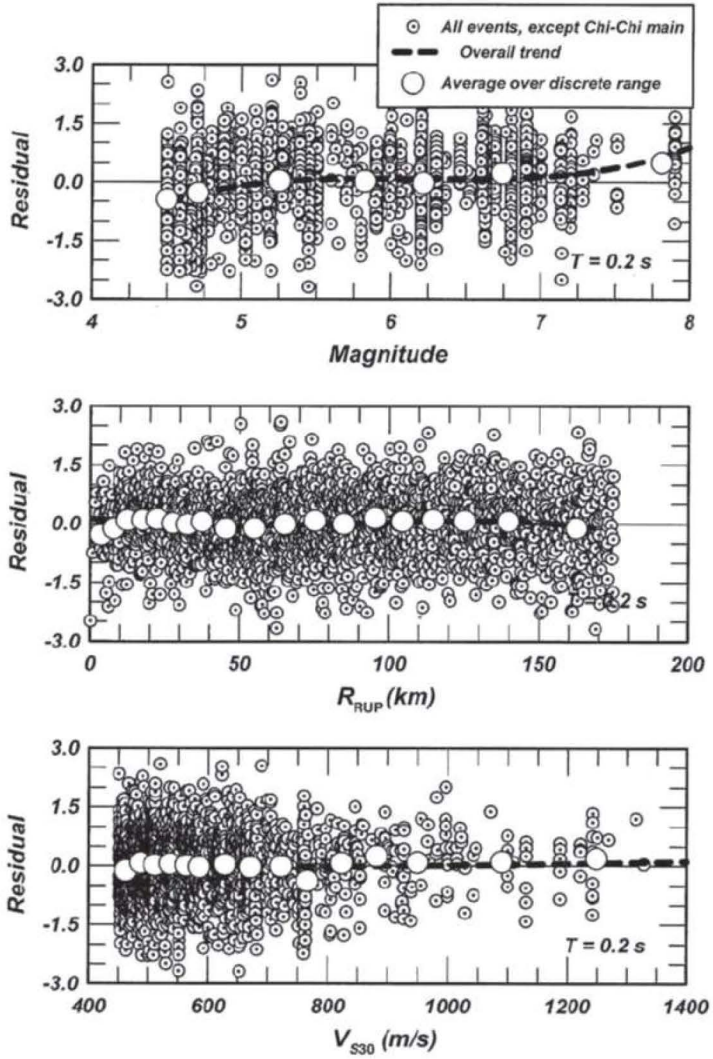

Figure 13. Residuals versus magnitude, rupture distance and V_{S30} using the derived equation for estimating PSA for $T = 0.2$ s at sites with $V_{S30} \geq 450$ m/s.

Standard error